RAIN-ON-SNOW IN THE EASTERN UNITED STATES AND ASSOCIATED SURFACE ENERGY BUDGET AND ATMOSPHERIC CIRCULATION

by

LORI JEAN WACHOWICZ

(Under the Direction of Thomas L. Mote)

ABSTRACT

Synoptic-scale atmospheric circulation can play a role in establishing dominant surface energy budget terms during large snow ablation events. This thesis links circulation with the energy budget during snow ablation that occurs during rainfall, i.e. rain-on-snow (ROS). First, several ROS identification criteria are compared to show variability across the eastern U.S. in order to establish a regional climatology of ROS events. Findings show variability in seasonal maximum and minimum ROS frequency depend on the criteria used. Second, the attributes of synoptic types, as derived from the Temporal Synoptic Index, are compared for ROS events. Results show the importance of sensible and latent heat advection. A one-dimensional snowpack model (SNTHERM) is used to model energy budget terms across common synoptic types. The sensitivity of the energy budget to rainfall is assessed, and results show the importance of changes in the snowpack thermal structure on heat introduced from the ground.

INDEX WORDS: Rain-on-snow, Snow ablation, Synoptic climatology

RAIN-ON-SNOW IN THE EASTERN UNITED STATES AND ASSOCIATED SURFACE ENERGY BUDGET AND ATMOSPHERIC CIRCULATION

by

LORI JEAN WACHOWICZ

B. S., Michigan State University, 2015

A Thesis Submitted to the Graduate Faculty of The University of Georgia in Partial Fulfillment of the Requirements for the Degree

MASTER OF SCIENCE

ATHENS, GEORGIA

2017

© 2017

Lori Jean Wachowicz

All Rights Reserved

RAIN-ON-SNOW IN THE EASTERN UNITED STATES AND ASSOCIATED SURFACE ENERGY BUDGET AND ATMOSPHERIC CIRCULATION

by

LORI JEAN WACHOWICZ

Major Professor:	Thomas L. Mote
Committee:	Andrew Grundstein Gina Henderson

Electronic Version Approved:

Suzanne Barbour
Dean of the Graduate School
The University of Georgia
December 2017

ACKNOWLEDGEMENTS

First, I gratefully acknowledge my advisor, Dr. Thomas Mote, for his patience and guidance in helping me work through my thesis. I would also like to acknowledge my committee members, Drs. Andrew Grundstein and Gina Henderson, for their additional support and feedback throughout the process of completing this thesis.

I am also grateful for the Department of Geography for providing a great support system for everything from helping fill out forms to inspiring me to conquer to new challenges in classes. Additionally, I owe various members of my cohort much gratitude for their emotional support and providing great memories that I will forever cherish. I especially thank members of the Climatology Research Lab for their guidance when I needed help with coursework or coding.

I would not have achieved this degree without the unconditional love and support given to me by my parents. They have never doubted my abilities and have always encouraged me to challenge myself. I am forever grateful for them.

Lastly, I thank to my adorable corgi, Radar. Without her, I probably would have never seen the light of day while writing this.

TABLE OF CONTENTS

Page

ACKNOWLEDGEMENTS iv

LIST OF TABLES vii

LIST OF FIGURES ix

CHAPTER

1 INTRODUCTION AND LITERATURE REVIEW 1

Overview 1

Motivation 2

Background 4

Research Objective 9

2 ESTABLISHING A RAIN ON SNOW CLIMATOLOGY IN THE EASTERN UNITED STATES 10

Introduction 12

Data and Methodology 13

Results 15

Conclusion 22

References 25

Tables and Figures 28

3 ASSESSING THE IMPACT OF RAIN ON THE SURFACE ENERGY BUDGET ON A SNOWPACK IN THE MID-ATLANTIC UNITED STATES 41

Introduction 43

Data and Methodology 44

Results 47

Conclusion 55

References 58

Tables and Figures 61

4 CONCLUSION 78

REFERENCES 81

LIST OF TABLES

Page

Table 2.1: Summary of different ROS studies, including in the study region and the environmental variable thresholds used to identify ROS events. 28

Table 2.2: Average temperature (°C), snow depth (cm), loss of snow depth (cm), and liquid equivalent of precipitation (cm) criteria used for ROS identification definitions. 29

Table 2.3: Total number of identified ROS events identified at Philadelphia, PA (KPHL), Buffalo, NY (KBUF), and Flint, MI (KFNT), as well as the seasonal totals for autumn (SON), winter (DJF), and spring (MAM). 30

Table 3.1: Common TSI synoptic type and descriptions associated with ROS dates from 1980 – 2009 at KPHL; total number of days of identified under the given synoptic type and percentage of the total in which ROS occurred are included.....61

Table 3.2: Average meteorological characteristics for each synoptic type from the TSI synoptic calendar and number of events (N) for 1949–2015 as well as the subset of ROS dates analyzed in this paper during 1980–2009; variables included are air temperature (T, ºC), dew point (Td, ºC), sea level pressure (SLP, hPa), u and v wind components (u, v, m s^{-1}), and cloud cover fraction (CC).....62

Table 3.3: Average daily flux components (W m^{-2}) and albedo (a) as well as modeled temperature (T, °C), relative humidity (RH, %) and wind speed (WS, m s^{-1}) for the common synoptic types associated with ROS for each event as well as an average for each synoptic type. 63

Table 3.4: Results from a single factor ANOVA for net shortwave radiation (Knet), net longwave radiation (Lnet), sensible (H), latent (LE), and ground (G) heat fluxes during ROS events 64

Table 3.5: Average daily flux components (W m^{-2}) and albedo as well as modeled temperature (T, °C), relative humidity (RH, %) and wind speed (WS, m s^{-1}) for the common synoptic types associated with each event after all precipitation is removed from the model run as well as an average for each synoptic type. 65

Table 3.6: Results from a paired sample for means t-Test for daily ground heat flux for Weak Carolinas Low (α=0.05) 66

Table 3.7: Results from a paired sample for means t-Test for daily ground heat flux for Great Lakes Low (α=0.05) 67

Table 3.8: Results from a paired sample for means t-Test for daily ground heat flux for Mid-Atlantic Coastal Low(α=0.05) 68

LIST OF FIGURES

Page

Figure 2.1: A topographic map of the eastern U.S. with the locations of the three sites (KPHL, KBUF, and KFNT) shown as red, blue, and yellow dots, respectively.....31

Figure 2.2: Number of days per year in which rainfall and a snowpack are present from September to May for (a) Any rainfall >0 cm, (b) a snowpack of > 0 cm, (c) any rainfall >1 cm, and (d) a snowpack >1 cm.....32

Figure 2.3: Average number of ROS events per year for (a) D1, (b) D2, (c) D3, and (d) D4.....33

Figure 2.4: Number of ROS events per season for autumn (SON) for (a) D1, (b) D2, (c) D3, and (d) D4 34

Figure 2.5: Number of ROS events per season for winter (DJF) for (a) D1, (b) D2, (c) D3, and (d) D4 35

Figure 2.6: Number of ROS events per season for spring (MAM) for (a) D1, (b) D2, (c) D3, and (d) D4 36

Figure 2.7: Average daily temperature in °C (a), daily snow depth in cm (b), change in snow depth in cm (c), and rainfall in cm (d) on ROS days at KPHL for each definition 37

Figure 2.8: Average daily temperature in °C (a), daily snow depth in cm (b), change in snow depth in cm (c), and rainfall in cm (d) on ROS days at KBUF for each definition.....38

Figure 2.9: Average daily temperature in °C (a), daily snow depth in cm (b), change in snow depth in cm (c), and rainfall in cm (d) on ROS days at KFNT for each definition 39

Figure 2.10: Time series of total counts per year for (a) Definition 1, (b) Definition 2, (c) Definition 3, and (d) Definition 4. 40
Figure 3.1: Composites of mean sea level pressure in hPa (black contours) and 500 hPa heights (filled contours) for a 00z to 00z period on ROS days for (a) the Mid-Atlantic Coastal Low (1032), (b) the Weak Carolinas Low (1004), (c) the New England Low (1011), and (d) the Great Lakes Low (1031).....69
Figure 3.2: Composites of precipitable water vapor in mm (filled contours) and 850 hPa heights (black contours) and 850 hPa wind speed in m s^{-1} for the 00z to 00z period on ROS days for (a) the Mid-Atlantic Coastal Low (1032), (b) the Weak Carolinas Low (1004), (c) the New England Low (1011), and (d) the Great Lakes Low (1031). 70
Figure 3.3: Average rainfall rates (mm hr^{-1}) for each synoptic type. Rainfall rates are estimated from MERRA-2 total precipitation land product minus total snowfall land product for (a) the Mid-Atlantic Coastal Low (1032), (b) the Weak Carolinas Low (1004), (c) the New England Low (1011), and (d) the Great Lakes Low (1031) 71
Figure 3.4: Average daily flux components for modeled rain (blue) and no-precipitation (red) events for the daily average (a) net shortwave radiative flux, (b) net longwave radiative flux, (c) sensible heat flux, (d) latent heat flux, and (e) ground heat flux (W m^{-2}).....72

Figure 3.5: Time series of 2-hour SNTHERM output for net shortwave radiation (W m^{-2}) for each ROS event (left column), the no-precipitation scenario (center column), and the difference between the two scenarios, calculated as R – NP (right column); rows are broken up by synoptic type with Weak Carolinas Low (1004; top), New England Low (1011; second from top), Great Lakes Low (1031; second from bottom), and Mid-Atlantic Coastal Low (1032; bottom). 73

Figure 3.6: Time series of 2-hour SNTHERM output for net longwave radiation (W m^{-2}) for each ROS event (left column), the no-precipitation scenario (center column), and the difference between the two scenarios, calculated as R – NP (right column); rows are broken up by synoptic type with Weak Carolinas Low (1004; top), New England Low (1011; second from top), Great Lakes Low (1031; second from bottom), and Mid-Atlantic Coastal Low (1032; bottom). 74

Figure 3.7: Time series of 2-hour SNTHERM output for sensible heat flux (W m^{-2}) for each ROS event (left column), the no-precipitation scenario (center column), and the difference between the two scenarios, calculated as R – NP (right column); rows are broken up by synoptic type with Weak Carolinas Low (1004; top), New England Low (1011; second from top), Great Lakes Low (1031; second from bottom), and Mid-Atlantic Coastal Low (1032; bottom). 75

Figure 3.8: Time series of 2-hour SNTHERM output for latent heat flux (W m^{-2}) for each ROS event (left column), the no-precipitation scenario (center column), and the difference between the two scenarios, calculated as R – NP (right column); rows are broken up by synoptic type with Weak Carolinas Low (1004; top), New England Low (1011; second from top), Great Lakes Low (1031; second from bottom), and Mid-Atlantic Coastal Low (1032; bottom). 76

Figure 3.9: Time series of 2-hour SNTHERM output for ground heat flux (W m^{-2}) for each ROS event (left column), the no-precipitation scenario (center column), and the difference between the two scenarios, calculated as R – NP (right column); rows are broken up by synoptic type with Weak Carolinas Low (1004; top), New England Low (1011; second from top), Great Lakes Low (1031; second from bottom), and Mid-Atlantic Coastal Low (1032; bottom). 77

CHAPTER 1

INTRODUCTION AND LITERATURE REVIEW

1.1. Overview

In areas where seasonal snow cover is present, the loss (ablation) of this snow cover depends on a variety of processes typically driven by air temperature and other factors such as wind and precipitation, which may enhance ablation. A subset of ablation events, known as "rain-on-snow" (ROS), are events where rain falls upon an existing snowpack, enhancing ablation rates and potentially producing damaging flooding. This happened when unusual synoptic conditions provided favorable conditions for the rapid ablation of a deep snowpack, later enhanced by rain, in January 1996 in the northeastern United States. This event caused an estimated $1.5 billion in damage as well as 30 fatalities in north-central Pennsylvania (Leathers et al. 1998).

Though infrequent, these ROS events have shown the potential to produce devastating floods, leading to loss of life especially in areas where topography can enhance runoff, such as mountainous areas (Graybeal and Leathers 2006; Ashley and Ashley 2008). In the higher latitudes, ROS has even been shown to affect wildlife populations by preventing them from reaching their food sources through means of hardening of snowpack (Putkonen et al. 2009). As these events are likely to occur in regions of higher latitude and elevation given a prominent seasonal snowpack, several studies including McCabe et al. (2007), Guan et al. (2016), and Jennings and Jones (2015), tend to focus on the impact of these events in the western United States. Other places throughout the world such as northern Eurasia and Germany (e.g., Ye et al.,

2008; Rössler et al., 2014; and Freudinger et al., 2014) have also been focused on. However, despite the significance of the 18–19 January 1996 snowmelt-flooding event in Pennsylvania, few studies have explicitly examined the impact of ROS in this region. Moreover, given the unusual synoptic conditions leading up to this event, the role of synoptic-scale circulation associated with ROS explicitly as well as its role in the melt process during these types of events has yet to be examined. Studies such as Grundstein and Leathers (1999) and Leathers et al. (2004) have established relationships between variations in circulation and snowmelt, though have not considered ROS explicitly as well. Therefore, this thesis has the potential to contribute to several gaps in the current literature through furthering our understanding of the physical mechanisms driving snowmelt during ROS.

1.2. Motivation

The eastern U.S., particularly in higher elevations and higher latitudes of the mid-Atlantic region, is subjected to large amounts of snowfall during its winter months. From a socio-economic standpoint, this region contains some of the highest population densities in the U.S., putting the lives and properties of many at risk if an event similar to that of January 1996 were to occur again.

Ashley and Ashley (2008) showed that snowmelt-induced flooding events, particularly from ROS, make up a large portion of flood-related deaths in the northeastern U.S. More importantly, while some areas of North America are expected to see a decrease in ROS events in the future due to the projected loss in snow cover (Jeong et al., 2017; Cohen et al., 2015), the Northeastern U.S. is expected to see increased ROS-induced runoff events due to a projected increase in rainfall (Jeong et al. 2017).

Furthermore, Frei et al. (2015) found that 80–90% of extreme streamflow events in the northeast U.S. occur during the winter, and are attributed to ROS. Even so, a comparison of the January 1996 ROS event with another ROS event in January 1978 in the same region (Kroczynski 2004) showed that differing hydrologic responses between individual ROS events is partially the result of snowpack characteristics. Jennings and Jones (2015) found that certain meteorological characteristics (e.g., dew point, wind speed, and precipitation) contribute to the snowpack outflow rate during ROS. More importantly, Jennings and Jones (2014) suggest the most extreme ROS events occur from steady rainfall and continued melt within the snowpack. As a result, identifying which meteorological variables drive the snowmelt process, regardless of varying snowpack characteristics, is necessary to improve the current understanding of hydrologic responses during ROS.

Collins et al. (2014) attempted to establish an association between flood-generating precipitation mechanisms at the synoptic scale by concluding that there is some relationship between flood magnitude and certain synoptic types. However, they did not examine all flood events, and left unanswered questions related to snowmelt and ROS-induced flooding. Again, the Collins et al. (2014) work provides motivation for understanding the larger-scale circulations and associated physical mechanisms driving the snowmelt process, particularly during ROS. An improved understanding of the snowmelt process during ROS may help improve current understanding and forecasting of future flooding events, particularly under future climate scenarios.

1.3. Background

1.3.1. Climatology

Several attempts at producing a climatology of ROS events have been published. Perhaps the most extensive seasonal climatology is that of Cohen et al. (2015), which examined frequencies of ROS across the Northern Hemisphere. Beyond the hemispheric scale, several regional-scale climatologies have been made, such as in the western United States (McCabe et al. 2007) and northern Eurasia (Ye et al. 2008). Furthermore, even sub-regional climatologies have been produced to exclusively examine ROS in areas such as the state of New York (Pradhanang et al. 2013), Germany (Freudiger et al. 2014), and the Sierra Nevada mountain range (Guan et al. 2016). The consensus of these results indicated the tendency for ROS events to depend on higher latitude and/or elevation, as these locations tend to experience greater snow cover. Furthermore, Garvelmann et al. (2014) indicated that elevation as well as aspect and vegetation can influence ROS events.

Seasonally, most ROS events occur during winter months in the northeastern U.S. (Cohen et al. 2015; Pradhanang et al. 2013), Germany (Freudiger et al. 2014), and Eurasia (Ye et al. 2008). Again, it is intuitive that more ROS events would occur during the months with a higher frequency of snow cover. Meanwhile, Guan et al. (2016) found that ROS events associated with filaments of high water vapor transport, known as atmospheric rivers (ARs), are more frequent during the month of March in the Sierra Nevada Mountains; however, McCabe et al. (2007) found ROS is generally most frequent in January over the entire western U.S. These differences in regional climatologies indicate a need for examining ROS and its properties on a sub-regional scale. More importantly, the aforementioned research completed on ROS used different data sources (reanalysis, station data, etc.) as well as different techniques to identify

individual events, and there is no published climatology of events for the northeastern U.S. – an area of complex terrain, seasonal snow cover, and a history of deadly snowmelt-related flooding.

1.3.2. Rain on snow and the surface energy budget

Ablation of a snowpack, including that from ROS, is dependent on a combination of meteorological and hydrological components, which is further enhanced based on the geography of the location of interest. Ablation is driven by the surface energy budget (SEB), which describes the various sources contributing energy to the snowpack, which is given by:

$$Q = S_{net}+L_{net}+H_s+H_l+H_p+G \quad (1)$$

where Q is the total energy contributing to ablation, S_{net} is the net shortwave radiation, L_{net} is the net longwave radiation, H_s is sensible heat flux, H_l is latent heat flux, H_p is energy flux from precipitation, and G is ground heat flux. In some cases, S_{net} typically dominates, particularly when air temperatures are above freezing and little cloud cover is present (Garvelmann et al. 2014). Turbulent fluxes, such as those from sensible and latent heat, tend to enhance the melting process during ROS, as these fluxes are dependent on warmer temperatures, higher dew point temperatures, and higher wind speeds (Garvelmann et al. 2014; Leathers et al. 2004). Positive sensible heat fluxes result when air temperatures above freezing tend to transfer heat energy into the snowpack through convection with the help of wind. Negative latent heat fluxes typically result in the evaporation of any snowmelt, particularly on colder, drier days; on the other hand, positive latent heat fluxes add heat through the condensation on the surface of the snowpack through higher dew point temperatures and wind (Leathers et al. 2004). Ground temperature and the presence of clouds can also contribute to melt by enhancing both G and L_{net}, though usually to a lesser degree.

ROS events may look quite different when examining the individual SEB terms. Nonetheless, many studies that examined the energy budget of ROS events failed to consider H_p — the heat flux due to the addition of precipitation into the snowpack. Though widely neglected in SEB calculations, H_p does occasionally contribute to Q during ROS events and therefore lead to higher potential snowmelt. One example is given by Mazurkiewicz et al. (2008), who compared snowmelt for ROS at different elevations. They found that turbulent exchanges (from sensible and latent heat) contribute most towards ROS-induced melt, with the H_p term contributing a significant portion (21%) towards the SEB during one particular event.

Garvelmann et al. (2014) compared individual energy fluxes during both ROS and non-ROS conditions. They determined that areas of no forest canopy have turbulent fluxes dominate both ROS and non-ROS conditions; conversely, for areas under a forested canopy both turbulent exchanges along with net longwave tend to dominate, though the magnitude of turbulent exchanges are much less than when no canopy is present. While the magnitude of H_p is small, Garvelmann et al. (2014) found that H_p is an important contribution of energy. Furthermore, an examination of six different ROS occurrences in the western U.S. by Jennings and Jones (2015) found that H_p can contribute to the SEB with the same magnitude as sensible and latent heat fluxes, particularly in instances where there is persistent rainfall.

On the contrary, an analysis of the modeled SEB associated with the 18–19 January 1996 event in Pennsylvania showed rain having little influence in the ablation process, despite as much as 7.5 cm of rain falling upon a deep snowpack. Given the importance of this event to the northeastern U.S. region, this case study was one of the few attempts at examining the relationship between synoptic scale circulation and ROS.

1.3.3. Role of Atmospheric Circulation

The spatial distribution of snow cover and the frequency and intensity of rainfall are both influenced by low-frequency patterns of mid-tropospheric circulation, commonly known as atmospheric teleconnections. Therefore, teleconnections should be related to the frequency and spatial distribution of ROS. Cohen et al. (2015) found that there is a higher frequency of ROS in the northeastern U.S. during a negative Arctic Oscillation (AO) phase due to more frequent snow cover. In northern Eurasia, the North Atlantic Oscillation (NAO) may be positively correlated to a higher frequency of ROS events (Cohen et al. 2015; Ye et al. 2008), though the exact reason behind this is not apparent (Ye et al. 2008). McCabe et al. (2007) suggests that in the western U.S., El Nino / Southern Oscillation (ENSO) accounts for some spatial variability in ROS events. Although Cohen et al. (2015) found no significant relationship with ENSO, they suggested ROS events occur less frequently in eastern North America and northern Europe during positive phases of the Pacific teleconnection patterns (e.g., Pacific Decadal Oscillation, Pacific/North American pattern, and ENSO) in general. This is likely the result of the Pacific Decadal Oscillation (PDO) supporting cooler and drier conditions in parts of the U.S. They also note an increase in events in the mid-Atlantic during positive PDO phases, which may be the result of cooler, but wetter winters in the more southern portions of the U.S.

Much research has been done examining the synoptic-scale environment associated with ablation, but little work has been published on the synoptic types or air mass types specific to ROS events. Leathers et al. (2004) found that variations in air mass types produce different dominant terms within the SEB during large ablation events. They concluded that sensible heat flux (H_s) typically dominates in a moist air mass, which could lead to a ROS-type of ablation event. Similarly, Grundstein and Leathers (1999) showed three synoptic-scale patterns typically

associated with large ablation events in the northern Great Plains region. They concluded that significant ablation occurred within the warm sector of a cyclone for all synoptic patterns, leading to sensible heat advection.

Occasionally an area of enhanced moisture transport within the warm sector of a mid-latitude cyclone is associated with an AR is present. ARs can provide added moisture and enhanced low-level winds at a location, with the potential to produce excess precipitation, through its interactions with local topography. Rössler et al. (2014) explained that one of the main contributors to an extreme ROS event in the Bernese Alps in Switzerland was an AR associated with an extra-tropical cyclone. Similarly, Guan et al. (2016) suggests that nearly 50% of ROS occurrences in the Sierra Nevada are caused by ARs.

While likely more common in some locations over others, ARs are not present with every synoptic-scale cyclone, though the warm air and moisture advection associated with the warm sector of the cyclone still plays an important role. In fact, the January 1996 event with another ROS event provides insight into snowmelt flood forecasting in this region by suggesting that the duration of strong wind and warm, moist air advection increases turbulent fluxes, aiding in snowpack ripening and thus determining the hydrologic consequences of an event (Kroczynski 2004; Anderson and Larsen 1996). Again, as these factors depend on the movement of synoptic-scale systems, as well as larger scale circulation, this suggests that variations in synoptic-scale patterns may be more conducive to ROS events. Furthermore, the extent of these atmospheric variables occurring within the warm sector of a cyclone have the potential to produce greater sensible and latent heat fluxes and in turn, possibly increasing potential melt.

1.4. Research Objective

Past research has shown linkages between synoptic-scale circulation and ablation of snow cover. Furthermore, studies have linked different circulation patterns to variations in the energy budget. However, fewer have attempted to establish a link between synoptic-scale circulation, the surface energy budget, and ablation, specifically considering rain-enhanced ablation. Therefore, the goals of this thesis are to establish a comprehensive climatology of ROS for the eastern US; to discern primary modes of synoptic-scale atmospheric circulation associated with ROS; and to relate these variations to the surface energy budget to address sensitivity of rainfall during ROS. More specifically the following questions are addressed:

- Is there a best way to identify ROS events throughout the eastern U.S., particularly the mid-Atlantic region? How do these different methodologies change the climatology of ROS?
- What is the SEB during ROS events? Is there variation in the SEB as a result of synoptic-scale circulation patterns commonly associated with ROS?
- How important is the rain during these events on the snowpack as well as the SEB? Does this impact vary between synoptic types?

CHAPTER 2

ESTABLISHING A RAIN ON SNOW CLIMATOLOGY IN THE EASTERN UNITED STATES[1]

[1] Wachowicz, L. and T. Mote. To be submitted to *Physical Geography*

Abstract

Rain-on-snow has the potential to produce devastating floods, as runoff from rain as well as the contribution of snowmelt can enhance flooding. While these events are most common in areas prone to extensive snow cover (i.e., higher latitudes and/or higher elevations), most rain-on-snow research has focused primarily in the western United States, despite the fact the eastern U.S. also experiences these events. Climatologies produced for the eastern U.S. have used primarily reanalysis data. This study uses a gridded snow dataset based on observations for a 50-year period (1960–2009) to establish a more comprehensive climatology for this region. Additionally, different methodologies used to identify events (using temperature, snow depth, and liquid water equivalent of precipitation) in this dataset are compared to demonstrate sensitivity of event selection when considering trends at Philadelphia, PA; Flint, MI; and Buffalo, NY.

Results show some spatial variability between definitions, particularly related to the snow and rainfall climatologies of the region. ROS events identified with strict rainfall criteria (>1 cm) are more frequent along the east coast; events identified with strict snow loss (>1 cm) are more common in higher latitudes and/or elevations. Seasonal variability exists, with most events occurring in the spring (MAM) and fewest in autumn (SON). Additionally, temporal trends at the three locations suggest that while Buffalo and Flint experience more events due to more days with snow cover there is an apparent decrease in ROS in these areas; no trend is apparent in Philadelphia. It is hypothesized large-scale teleconnections, such as the Arctic Oscillation, play a role on a regional scale, but localized impacts should be considered with future work.

Key Words: Rain-on-snow, Snow ablation, Eastern US

2.1 Introduction

The seasonal snowpack of the eastern United States is important for regional hydrology, as it serves as a source for replenishing groundwater during the melt season. The spatial and temporal extent of this snowfall depends on factors such as geography (e.g., latitude and elevation) and climatology (e.g., temperatures, rainfall and snowfall) of the area. These factors can act to enhance the timing and amount of melt of the seasonal snowpack, particularly in instances of warmer temperatures and/or the presence of rainfall. These instances where rain falls on a snowpack, known as "rain-on-snow" (ROS), the rain can potentially contribute to significant flooding, particularly in high elevations (McCabe et al. 2007; Marks et al. 1998), which can impact life and property.

For example, a rapid snowmelt event in January 1996 in central Pennsylvania caused significant damage to properties estimated at $1.5 billion and took the lives of more than 30 people (Leathers et al. 1998). This event is important given the 7 cm of rain which fell on a deep snowpack. Additionally, in the northeastern and mid-Atlantic regions of the US, most deaths from flooding are the result of snowmelt-induced floods (Ashley and Ashley 2008). These numbers can potentially increase in the future given the projected increase in runoff events resulting from ROS, despite fewer total ROS events (Jeong et al. 2017; Cohen et al. 2015).

Current climatologies of ROS have been established on scales ranging from hemispheric (Cohen et al. 2015), to continental (e.g., McCabe et al. 2007; Ye et al. 2008), to regional (e.g., Pradhanang et al. 2013; Freudiger et al. 2014; Guan et al. 2016). Within all of these domains, ROS tends to be dependent on latitude and elevation, given the availability of snow cover. Land cover, such as the presence of vegetation, can likewise play a role in ROS predictability (Garvelmann et al. 2014). Most ROS events tend to occur during winter months (DJF),

especially in the northeastern U.S. (Cohen et al. 2015; Pradhanang et al. 2013), Germany (Freudiger et al. 2014), and northern Eurasia (Ye et al. 2008) given the higher frequency of snow cover.

A comprehensive climatology of ROS has not been established specifically for the eastern portion of the U.S., containing both the northeastern and mid-Atlantic regions. Climatological analyses using either reanalysis data or future model projections have been used to mostly look at hemispheric trends in ROS, few results specific to the northeastern and mid-Atlantic regions (Cohen et al. 2015; Jeong et al. 2017). Pradhanang et al. (2013) used in situ measurements, but were limited to only the state of New York. Additionally, each climatology paper identified ROS using different selection criteria, which may result in small discrepancies when comparing across studies. Therefore, the primary goals of this paper are to: (1) assess the sensitivity of event selection criteria on developing a ROS climatology, and use this to (2) develop a more comprehensive ROS climatology for the eastern US in terms of spatial and temporal trends.

2.2 Data and Methodology

ROS events are identified using the Daily Gridded North American Snow, Temperature, and Precipitation Dataset (Kluver et al. 2016; Dyer and Mote 2006). This is a daily gridded data set containing snow cover (m), temperature (°C), and precipitation (mm) interpolated from daily observations throughout the United States and Canada to a 1° x 1° grid. These data are available daily from 1900–2009, though only data from 1960 is used here to identify ROS due to documented data inconsistencies prior to 1960. Moreover, this dataset has been used in several snow-related studies (e.g., Suriano and Leathers 2017; Kluver et al. 2016; Leathers et al. 2004;

among others). In this study, we use maximum and minimum temperature (to calculate a daily average temperature), snow depth, and rainfall to identify ROS events.

Given the wide variety of criteria used in selected events in other ROS studies, several different definitions were selected and compared in terms of spatial and temporal patterns to discern major variations between definitions. As most literature broadly defines ROS as "rain falling on a snowpack," a summary of samples of ROS work show how differently each project identifies these events (Table 2.1). As a result, more than one definition (i.e., D1, D2, D3, D4) is assessed in this paper to provide insight on the importance of selection criteria in establishing a regional climatology (Table 2.2). ROS events are first identified using a definition (D1) in which the average daily temperature is above freezing (> 0 °C), there is snow on the ground (> 0 m), any measurable loss in snow depth (> 0 cm), and "rain" is present (> 0 cm); this definition is considered a "broadly-defined event." From there, a more rain-specific definition is developed (> 1 cm rainfall; D2) as well as a rapid loss in snow depth (> 0 cm; D3). Finally, a ROS event defined by both heavy rainfall (> 1 cm) and rapid snow loss (> 1 cm) for is included for D4. The definitions were selected based on a sample of different rainfall and snow depth thresholds from Table 2.1. Furthermore, given the available variables in the gridded dataset, no definitions are included using snow water equivalent and/or runoff. Any grid cell in which any of these criteria are met is included as a "ROS event" for a domain including the eastern U.S.

Additionally, we examine three cities with different winter conditions due to their latitude, elevation, and relative location to major bodies of water (Figure 2.1). ROS events are extracted for Philadelphia, PA (KPHL; 39.87ºN, 75.23ºW), Buffalo, NY (KBUF; 42.94ºN, 78.74ºW), and Flint, MI (KFNT; 42.97ºN, 83.75ºW) for each of the four aforementioned definitions and compared to assess temporal trends in ROS at each location.

2.3 Results

2.3.1 Spatial Variations by year

Spatial distributions of the number of days (September – May) per year (from 1960-2009) in which rainfall >0 cm (Figure 2.2a) and rainfall >1 cm (Figure 2.2c) occur; Figure 2.2b and Figure 2.2d show the number of days per year in which > 0 cm and >1 cm of snow cover is present, respectively. It is evident lower latitudes and/or lower elevations experience more rainfall days per year than higher latitudes and/or higher elevations. An inverse pattern is evident for days with a snowpack present, as higher latitudes and higher elevations tend to have more days per year with a snowpack present. Furthermore, there are fewer days in which >1 cm of rainfall is observed and fewer days in which a snowpack depth >1 cm is observed.

The average number of ROS events per year (including all 12 months) is presented in Figure 2.3. As D1 (Fig. 2.3a) provides the most inclusive criteria used to identify events, a higher frequency of these types of events is present, when compared to the average number of events for the other definitions (Figures 2.3b, 2.3c, 2.3d). More events per year were recorded using D1, particularly in northern Vermont and New Hampshire as snow cover is more frequent here (Figures 2.2b, 2.2c)., with as many as 30 or more events occurring per year. Additionally, a localized maxima is evident in West Virginia due to the topography in this region. Western New York state has a localized maxima possibly as the result of Lake Erie and Lake Ontario providing localized moisture, especially during autumn and early winter.

It is possible that using such an inclusive definition, though allowing for a better sample of events for further analysis, would include more spurious (or more-localized) events than using a stricter definition, which may include more spatially contiguous events. Therefore, additional definitions of ROS were examined. Those events with the stricter rain criteria (Figure 2.3b) with

minimal snow depth loss may indicate the addition of snow water equivalent into the pack.

A noticeable change in frequency of events is apparent for those events with the stricter snow depth criteria (Figures 2.3c, 2.3d) when compared to the frequency of D1 events. Local maxima were present in similar areas for D3 (Figure 2.3c) as for D1, indicating that local topography, such as elevation, may be playing a role regarding magnitude of snow depth loss, as higher elevation areas are more likely to have a deeper snowpack (Figure 2.2d). In fact, using this definition captured nearly half the amount of events as the most inclusive definition, which may help to reduce the number of spurious events, but may be including events not impacted by large amounts of rainfall.

Lastly, the fourth definition (Figure 2.3d) captured few events (< 5 events) occurring per year, with the majority of these occurring in higher elevations in upstate New York or along the coastline up in Maine, Vermont, and New Hampshire. These events tend to occur in areas where higher rainfall amounts are more common (Figure 2.2c).

2.3.2 Spatial Variations by season

2.3.2.1 Autumn

Seasonally across all definitions, autumn (SON) had fewer total ROS events per season (Figure 2.4) than winter (Figure 2.5) and spring (Figure 2.6). Events matching criteria set in D1 (Figure 2.4a) showed similar localized maxima as the average number per year (Figure 2.3) with as many as six seasonal events occurring in SON over a 50-year period. Additionally, local topographic influences contributed to the higher number of events occurring as a result of higher elevation.

Similar maxima were present from D2 (Figure 2.4b), indicating that ROS events identified with heavier rainfall may result from the interaction between atmospheric moisture and

local topography. A pattern of more events occurring along the mountains was evident, with 30 or more total events occurring from the Adirondack mountains northward. Additionally, higher elevations in West Virginia contributed to the southward extent of total events. Relatively few events (less than one per season) occurred west of the Appalachian mountains.

More ROS events were present in the far north using D3 (Figure 2.4c), with most events extending into Canada. Additional localized maxima occurred in areas close to Lakes Erie and Ontario, in which more frequent snow cover allows more ROS events to occur. This is supported by the distribution of events meeting D4 (Figure 2.4d), in which most events occur within the Adirondack area or further north. Additionally, although events under D4 are quite rare (less than one per season), these events are more likely to occur near the coastline, particularly up near Maine.

2.3.2.2 Winter

Similarly, in winter (DJF) months (Figure 2.5), more events were present when using D1 (Figure 2.5a), with localized maxima occurring in West Virginia, along the coast between New Jersey and Connecticut, as well as the maxima identified before between Lakes Erie and Ontario. More events occurred west of the Appalachian mountains in the winter, with areas in Michigan experiencing more than 6 events per season. Similar spatial patterns occur with events matching the D3 criteria (Figure 2.5c), suggesting that ROS events with little rainfall (<1 cm) were more common in these areas. Moreover, other factors may come into play regarding the loss of snow depth, as the areas of higher elevation as well as the Great Lakes region have a more persistent snowpack due to more snowfall than rainfall this time of year.

Perhaps most interestingly in the winter, localized maxima were present along the East Coast in which events with greater than 1 cm of rainfall were more common for both D2 and D4

(Figures 2.5b and 2.5d, respectively). This is likely the result of a less persistent and shallower snowpack during the winter, due to winter precipitation to falling more frequently as rain. ROS events meeting D4 were also most common closer to the coastline, with localized maxima occurring leeward of Lakes Huron and Ontario. Moreover, in both of these areas, at least one event occurs per season.

2.3.2.3 Spring

Most ROS events occur during the spring months (MAM), with localized maxima with totals much higher than in autumn and winter (Figure 2.6). Most ROS events identified using D1 tended to be located in areas of higher elevation as well as higher latitudes (Figure 2.6a). Particularly interesting is the maxima occurring in northern New Hampshire and Vermont, in which 24 or more events occur per season. It is possible localized ROS events tended to occur in this area, particularly in part of the geography of this area (e.g., high elevations) in the transitional seasons. Additionally, most ROS events in which snow depth loss (D3) was most prominent tended to occur in the northern latitudes, with more than six events per season (Figure 2.6c). This definition shows more events (>10 per season) in high elevation locations. Localized maxima were not as prominent as in the D1 cases likely because this definition includes more events that are widespread.

Similar to the patterns seen in the winter months, stricter rainfall criteria from D2 indicated as many as two or more events occurring close to the coastline (Figure 2.6b). Furthermore, ROS events categorized by D4 occur in this same area (Figure 2.6d), as well as events occurring in up-state New York, likely as the result of local topography (such as the Adirondacks) allowing for a sustained snowpack at higher elevations longer into the season. Additionally, ROS was less common for all definitions west of the Appalachian mountains, as snow cover is not as common, particularly late in spring.

2.3.3 Temporal variations

2.3.3.1 Meteorological Characteristics on ROS days

Total ROS counts under each definition are shown in Table 2.3 for three different locations: KPHL, KBUF, and KFNT. KBUF consistently experienced more ROS events, with most events occurring during winter and spring seasons. This is likely due to its placement near Lake Erie and Ontario, which allow for a snowpack being present for a longer duration during the year given the availability of lake effect snow, as well as rain in autumn months before the lakes freeze. Of these events broadly defined using D1, only about 6.7% of these (46 events identified using D4) are more "extreme" in terms of both loss of snow depth and rainfall amounts compared to those identified with D1, D2, or D3.

ROS events identified from D4 constituted about 5.1% of all ROS events identified for KFNT. Like KBUF, although ROS was more common when being identified using D1, much fewer events resulted when additional criteria were added (i.e., D2 and D3). Fewer events were identified with D2, D3, and D4 likely due to the location being more conducive to a snowpack presence longer during the year and climatologically less rainfall occurring particularly in the winter months.

Around 12.5% of all ROS events identified at KPHL from 1960–2009 were further identified using D4. Although ROS was more uncommon at KPHL in terms of total number of events, more of these events are considered to be attributed to higher rainfall amounts and result in more loss in snow depth when compared to KBUF and KFNT. This could indicate KPHL experienced a non-continuous snowpack as rain events are more common (Figure 2.2).

At KPHL, a breakdown of frequency in meteorological characteristics used to identify events (i.e., average daily temperature, snow depth, loss in snow depth, and precipitation) showed that most events identified using D1 and D3 were 1–4 °C above freezing during the day (Figure 2.7a). Events with stricter precipitation thresholds (i.e., D2 and D4) have a higher median temperature of near 1°C when compared to events identified using D1 and D3. Observed snow depth on most ROS days were typically 5 cm or less across all definitions (Figure 2.7b). Definitions sensitive to snow depth loss, particularly D3, more commonly observed greater snow depths than those events sensitive to rainfall or rain and snow depth loss (D2 and D4). The shallow observed snow depths could be attributed to ablation leading up to the ROS event. Not surprisingly, most ROS cases experienced a loss in snow depth of 1 cm or less across definitions with events identified with D3 and D4 consisting of a median snow depth loss near 2 cm (Figure 2.7c). Given the observed snow depth on ROS days to be under 5 cm (Figure 2.7b), this is to be expected. Moreover, in most ROS cases at KPHL, few are considered large ablation events, where these large events are shown via the outliers across definitions. Lastly, rainfall amounts of 1 cm or less tended to dominate ROS events identified with D1 and D3, shown by Figure 2.7d. Additionally, while it was most common for events using D2 to consist of 1–2 cm of rainfall, these higher rainfall amounts were also present in events under D4.

ROS events at KBUF categorized by D1 and D3 were typically associated with daily median temperatures near 2 °C above freezing (Figure 2.8a). Events with heavier rainfall (i.e., D2 and D4) had daily average temperatures near 2.5 °C in most cases. ROS events at KBUF across definitions typically had 10 cm or less snow depth (Figure 2.8b). Additionally, most ROS events experienced a loss in snow depth of 5 cm or less, with events categorized under D2 commonly resulting in snow depth losses of around 1–3 cm (Figure 2.8c). Rainfall amounts were typically 1–2 cm total for D2 and D4 events, and were much lower (< 0.5 cm) for events categorized under D1 and D3 (Figure 2.8d).

Lastly, ROS events at KFNT were similarly characterized by median daily temperatures near 2 °C across all definitions, with ranges of daily temperatures commonly 1 – 4 °C (Figure 2.9a). Additionally, most events that met D4 criteria had daily average temperatures near or above 2 °C. Snow depth characteristics of ROS at KFNT show that events occurred with shallow snowpacks of 5 cm or less (Figure 2.9b). This in turn led to loss of a snow depth of 1 cm or less for events identified with D1 or D2, suggesting most of these types of events could ablate the shallow snowpack (Figure 2.9c). Furthermore, rainfall amounts of 0.05 cm or less were common among ROS events categorized under D1 and D3 with rainfall amounts over 1 – 1.5 cm for ROS events under D2 and D4 (Figure 2.9d).

2.3.4 Yearly Trends in ROS Occurrences

Lastly, time series of the total number of events per year at the different locations (Figure 2.10). When comparing the different locations, similar trends in D1 ROS events, in which at KPHL and KBUF, the number of events per year tend to show a decline from 1960 onward; a decline in number of events per year is apparent at KFNT from about 1970 onward (Figure 2.10a). However, during 1970–1980, KFNT had more than 20 events while KPHL had much fewer (less

than 5). While the total number of events dropped around 2005 for both KPHL and KFNT, KBUF had more events in the late 2000s. Similar to D1, KFNT and KBUF had a decrease in ROS events that met D3 criteria from the mid-1970s until the mid-1990s, with numbers increasing slightly until 2009 (Figure 2.10c). KPHL had no apparent trend, although an increase in total numbers around 2002 occurred.

KBUF had more ROS events matching the D2 criteria prior to 1980, with total numbers per year decreasing to 4 or fewer for the remainder of the period (Figure 2.10b). KFNT experiences the fewest ROS events under D2. Additionally, KPHL and KFNT experienced D4 events less frequently (Figure 2.10d) than KBUF. However, while KBUF did not have as many of these events in total, there is an apparent trend in the number of these events over time, suggesting these events, while rare, may not be occurring as frequently.

The inter-annual variability in ROS at different locations is likely caused by teleconnection patterns, such as the Arctic Oscillation (AO), as analyzed by Cohen et al. (2015). Given the negative phase of the AO to result in colder temperatures and more snowfall in the northeastern portion of the U.S, more ROS events are likely to occur. While Cohen et al. (2015) found correlations between seasonal ROS and the AO in this region, local-scale variations likely also occur and should be considered with future work. Furthermore, long-term trends, particularly at KBUF and KFNT, are similar to those found by Suriano and Leathers (2017), in which changes in seasonal snow cover in this area is thought to be attributed to decreased frequency of ablation events in the Great Lakes region.

2.4 Conclusion

Rain-on-snow producing snowmelt can potentially cause damaging floods in areas of higher elevation and in areas with a seasonal snowpack. Rapid melting of the snowpack in parts

of the eastern U.S. has resulted in loss of life; therefore, assessing where these types of events are most common in this region may have assist in planning for these events. After comparing several different definitions to identify ROS in the eastern U.S., we can draw the following conclusions:

1. Differences among definitions result in varying number of ROS events per year. These different definitions exhibit local maxima which change depending on the criteria used. Definitions in which rainfall is an important factor shifted maxima toward the coastline. Definitions with stricter snow depth loss criteria shifted the maxima northward and further inland.
2. Seasonal differences occur among the definitions. More events tend to be present in spring, particularly for definitions focusing on snow loss (D3). Additionally, more localized maxima were present in fall and spring, likely due to identification of spurious events, particularly for D1, whereas stricter criteria (such as D4), showed a smoother spatial distribution of events through all seasons, indicating more widespread events.
3. Although KPHL experienced the least number of ROS events compared to KBUF and KFNT, a higher percentage of D4 events occurred at KPHL. The location of Philadelphia relative to the east coast likely allows for higher temperatures and enhanced moisture to play a role in producing more of these types of events.
4. Trends in frequency of events were present, particularly when using a more inclusive definition for KBUF and KFNT. There was no apparent trend in ROS in KPHL, likely due to a lower frequency of ROS in this area. These trends on a local scale could be the forcing of larger teleconnection patterns (e.g., Arctic Oscillation) and should be examined further with future work.

This analysis has shown that methodology in selecting events plays some role in establishing a more comprehensive climatology in this region, particularly in terms of individual locations and specific numbers. As a result, the subregional variation as a function of event selection suggests that ROS research focused on regional patterns (both spatial and temporal) may want to consider a broader, less-selective definition. Subregional and local studies should incorporate local climatology (e.g., temperature, snow depth, and precipitation) into selecting ROS events for analysis. Additionally, future work should consider the impact of these definitions in terms of runoff as a result of ROS, given the suggested increase of ROS-induced runoff in future climate scenarios in this region (Jeong et al. 2017).

2.5 References

Ashley, S. T. and W. S. Ashley, 2008: The storm morphology of deadly flooding events in the United States. *Int. J. Climatol*., **28**, 493–503, doi:10.1002/joc.1554.

Cohen, J., H. Ye, and J. Jones, 2015: Trends and variability in rain-on-snow events, *Geophys. Res. Lett.,* **42**, 7115–7122, doi:10.1002/2015GL065320.

Collins, M. J., J. P. Kirk, J. Pettit, A. T. DeGaetano, M. S. McCown, T. C. Peterson, T. N. Means, and X. Zhang, 2014: Annual floods in New England (USA) and Atlantic Canada: synoptic climatology and generating mechanisms, *Phys. Geogr.*, **35**, 195-219.

Dyer, J. L., and T. L. Mote, 2006: Spatial variability and trends in observed snow depth over North America. *Geophys. Res. Lett*., **33**, L16503, doi:10.1029/2006GL027258.

Freudiger, D., I. Kohn, K. Stahl, and M. Weiler, 2014: Large-scale analysis of changing frequencies of rain-on-snow events with flood-generation potential, *Hydrol. Earth Syst. Sci.,* **18**, 2695-2709.

Garvelmann, J., S. Pohl, and M. Weiler, 2014: Variability of observed energy fluxes during rain-on-snow and clear sky snowmelt in a midlatitude mountain environment, *J. of Hydrometeor.,* **15**, 1220-1237.

Graybeal, D. Y., and D. J. Leathers, 2006: Snowmelt-related flood risk in Appalachia: first estimates from a historical snow climatology, *J. of Appl. Meteor. Climatol.,* **45**, 178-193.

Guan, B., D. E. Waliser, F. M. Ralph, E. J. Fetzer, and P. J. Neiman, 2016: Hydrometeorological Characteristics of Rain-on-Snow Events Associated with Atmospheric Rivers, *Geophys. Res. Lett.,* **43**, 2964-2973.

Jennings, K. and J. A. Jones, 2015: Precipitation-snowmelt timing and snowmelt augmentation of large peak flow events, western Cascades, Oregon, *Water Resour. Res.*, **51**, 7649-7661.

Jeong, D. I., and L. Sushama, 2017: Rain-on-snow events over North America based on two Canadian regional climate models, *Clim. Dyn.*, 1-14.

Kluver, D., T. Mote, D. Leathers, G. R. Henderson, W. Chan, and D. A. Robinson, 2016: Creation and validation of a comprehensive 1 by 1 daily gridded North American dataset for 1900–2009: snowfall. *J. Atmos. Oceanic Technol.*, **33**, 857-871.

Leathers, D. J., D. Graybeal, T. Mote, A. Grundstein, and D. Robinson, 2004: The role of airmass types and surface energy fluxes in snow cover ablation in the central Appalachians, *J. of Appl. Meteor. Climatol.,* **43**, 1887-1899.

Leathers, D. J., D. R. Kluck, and S. Kroczynski, 1998: The severe flooding event of January 1996 across north-central Pennsylvania, *Bull. Am. Meteor. Soc.,* **79**, 785.

Marks, D., J. Kimball, D. Tingey, and T. Link, 1998: The sensitivity of snowmelt processes to climate conditions and forest cover during rain-on-snow: a case study of the 1996 Pacific Northwest flood, *Hydrol. Process*., **12**, 1569-1587.

McCabe, G. J., L. E. Hay, and M. P. Clark, 2007: Rain-on-Snow Events in the Western United States., *Bull. Amer. Meteor. Soc*., **88**, 319–328. doi: 10.1175/BAMS-88-3-319.

Mazurkiewicz, A. B., D. G. Callery, and J. J. McDonnell, 2008: Assessing the controls of the snow energy balance and water available for runoff in a rain-on-snow environment, *J. Hydrol.*, **354**, 1-14.

Pradhanang, S. M., A. Frei, M. Zion, E. M. Schneiderman, T. S. Steenhuis, and D. Pierson, 2013: Rain-on-snow runoff events in New York. *Hydrol. Process.*, **27**, 3035-3049.

Surfleet, C. G., and D. Tullos, 2013: Variability in effect of climate change on rain-on-snow peak flow events in a temperate climate, *J. Hydrol.*, **479,** 24-34.

Suriano, Z. J., and D. J. Leathers, 2017: Spatiotemporal Variability of Great Lakes Basin Snow Cover Ablation Events, *Hydrol. Process.,* 1–9.

Ye, H., D. Yang, and D. Robinson, 2008: Winter rain on snow and its association with air temperature in northern Eurasia, *Hydrol. Process.*, **22**, 2728-2736.

2.6 Tables and Figures

Table 2.1. Summary of different ROS studies, including in the study region and the environmental variable thresholds used to identify ROS events.

Source	Study Region	Definition used for identification of ROS event
Cohen et al. (2015)	Northern Hemisphere	Snow cover fraction > 0.5 and any liquid precipitation > 1 cm identified in grid cell.
Collins et al. (2014)	New England, US	Rainfall associated with any decrease in snow depth that occurred over a 3-day period or if snowfall occurred with no increase in snow depth; did not count events if snowmelt had been documented leading up to identified event.
Freudiger et al. (2014)	Germany	At least 3 mm of rainfall over a snowpack with at least 10 mm of SWE where "the sum of rainfall and snowmelt contains a minimum of 20% snowmelt" over at least one day.
Guan et al. (2016)	Sierra Nevada Mtn Range, US	>1 cm of precipitation calls during the day with a simultaneous reduction in SWE occurring at least at 3 different SNOTEL stations within a 200 km zonal band.
Jennings and Jones (2015)	W. Cascade Mtns., OR, US	3-day precipitation totals with > 150 mm and/or peak stream flow greater than 3.3 mm/hr [all events identified also had initial SWE > 0 with 60% precipitation falling as rain (not used as selection criteria)].
Jeong et al. (2017)	North America	Precipitation and SWE are > 1 mm and SWE decreases "following the definition of McCabe et al. (2007) and Surfleet and Tullos (2013)."
Mazurkiewicz et al. (2008)	W. Cascade Mtns., OR, US	24 hours (8 3-hr consecutive time steps) with more at least 0.254 mm of rain falls on the snowpack.
McCabe et al. (2007)	Western US	Any precipitation falling during a day that results in snow depth decrease.
Pradhanang et al. (2013)	New York, US	When any precipitation identified as rain falls on the snowpack, resulting in runoff.
Surfleet and Tullos (2013)	Oregon, US	Observed precipitation (amount not specified), maximum daily temperature > 0 C with a decrease in SWE.
Ye et al. (2008)	Eurasia	Any occurrence of liquid precipitation (denoted by various codes, depending on precipitation type) documented for at least one of the four daily observation periods.

Table 2.2. Average temperature (°C), snow depth (cm), loss of snow depth (cm), and liquid equivalent of precipitation (cm) criteria used for ROS identification definitions.

	Avg Temperature	Snow Depth	Snow Depth loss	Precipitation
D1	> 0 °C	> 0 cm	> 0 cm	> 0 cm
D2	> 0 °C	> 0 cm	> 0 cm	> 1 cm
D3	> 0 °C	> 1 cm	> 1 cm	> 0 cm
D4	> 0 °C	> 1 cm	> 1 cm	> 1 cm

Table 2.3. Total number of identified ROS events identified at Philadelphia, PA (KPHL), Buffalo, NY (KBUF), and Flint, MI (KFNT), as well as the seasonal totals for autumn (SON), winter (DJF), and spring (MAM).

		D1	D2	D3	D4
KPHL	Total	257	79	98	32
	SON	7	2	1	0
	DJF	193	57	76	24
	MAM	57	20	21	8
KBUF	Total	690	89	395	46
	SON	128	20	63	12
	DJF	290	30	186	11
	MAM	272	39	146	23
KFNT	Total	492	58	211	25
	SON	61	4	18	0
	DJF	274	38	127	17
	MAM	157	16	66	8

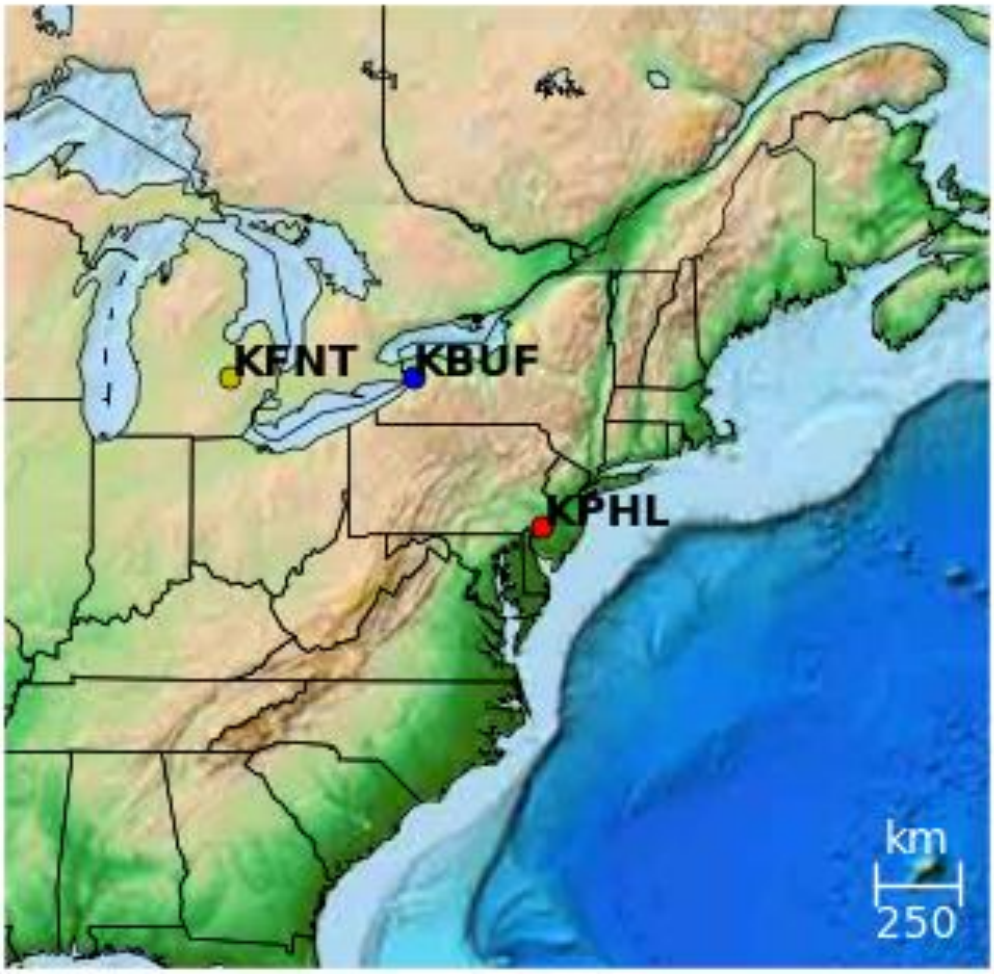

Figure 2.1. A topographic map of the eastern U.S. with the locations of the three sites (KPHL, KBUF, and KFNT) shown as red, blue, and yellow dots, respectively. Darker brown represents areas of higher elevation with green representing lower elevation and blue representing bodies of water.

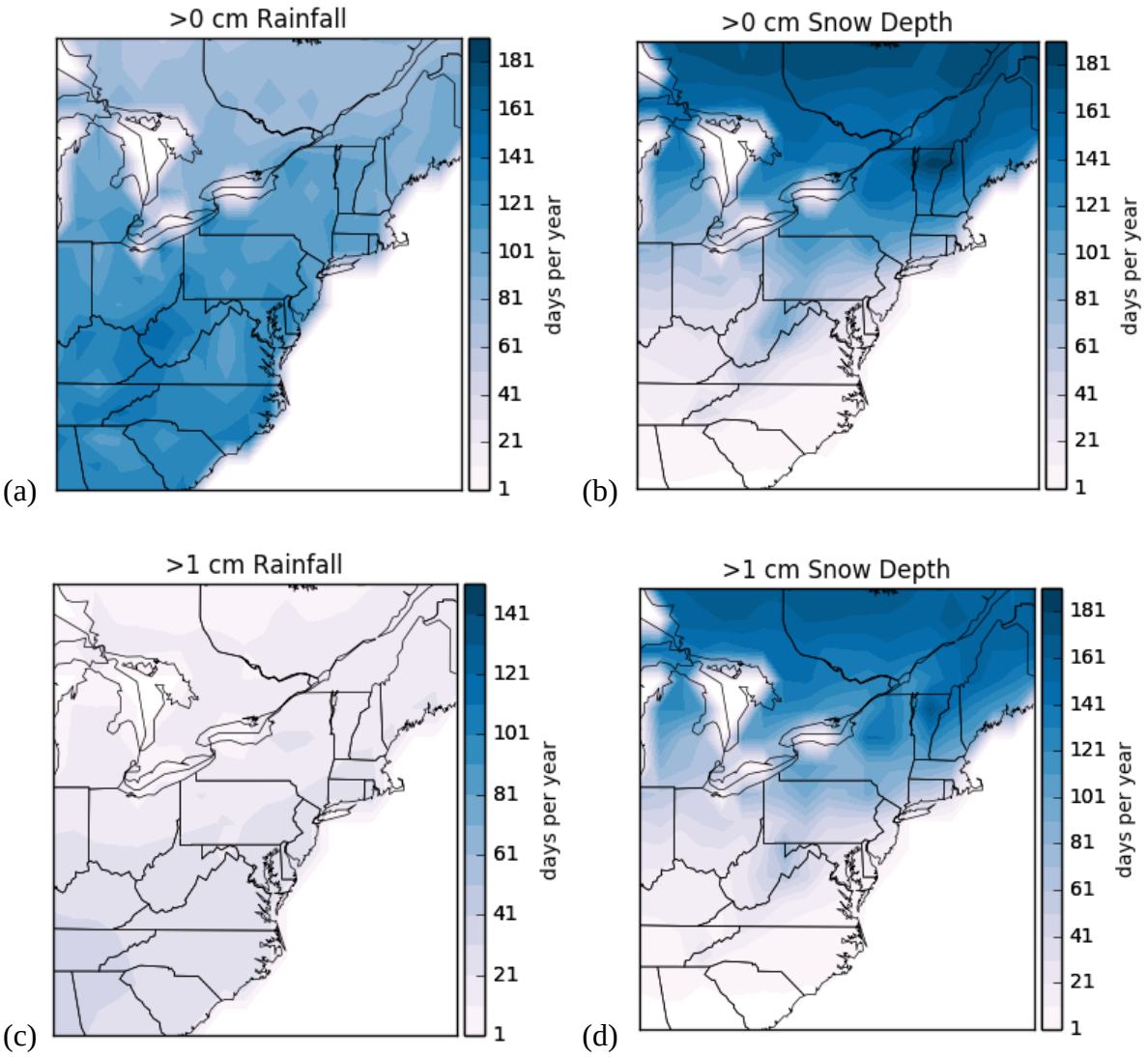

Figure 2.2. Number of days per year in which rainfall and a snowpack are present from September to May for (a) Any rainfall >0 cm, (b) a snowpack of > 0 cm, (c) any rainfall >1 cm, and (d) a snowpack >1 cm.

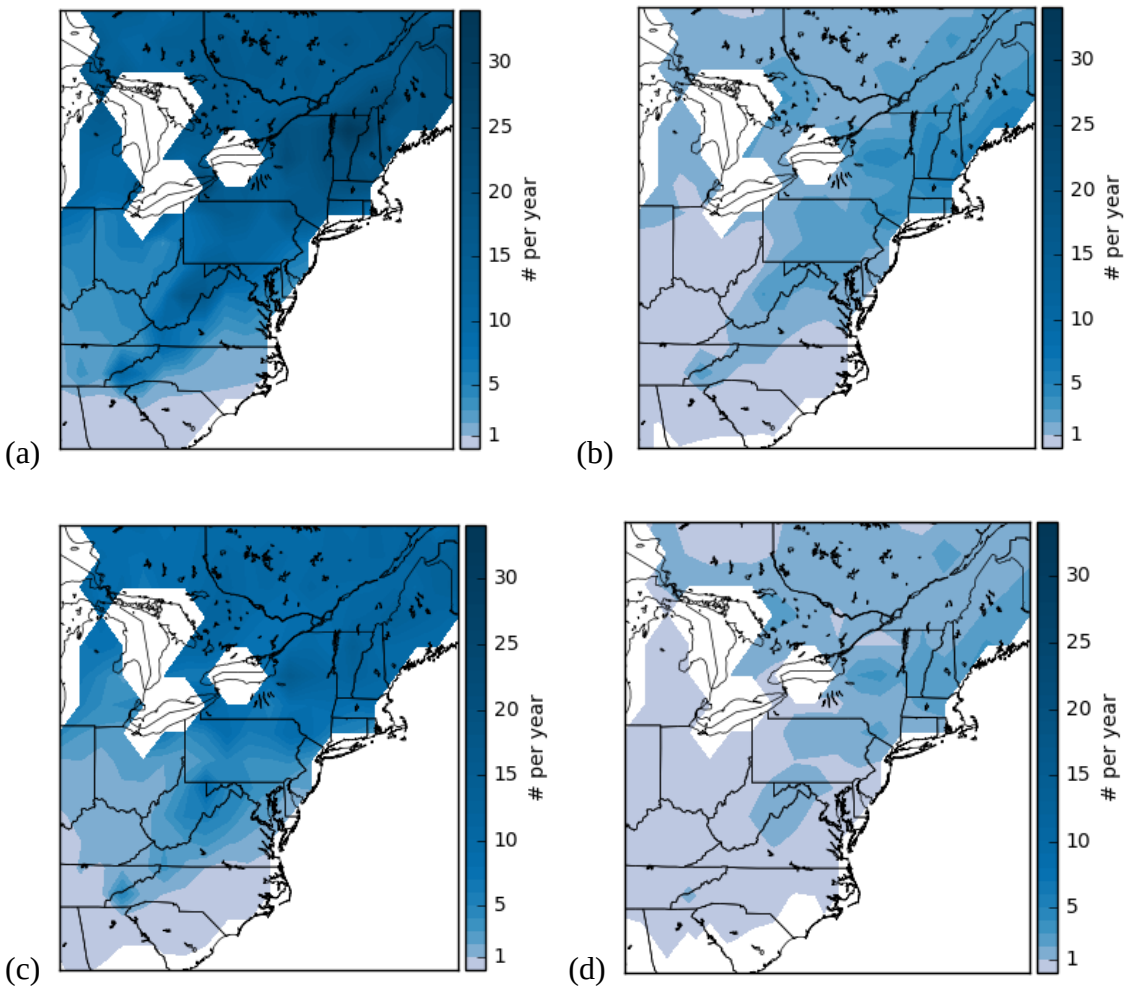

Figure 2.3. Average number of ROS events per year for (a) D1, (b) D2, (c) D3, and (d) D4.

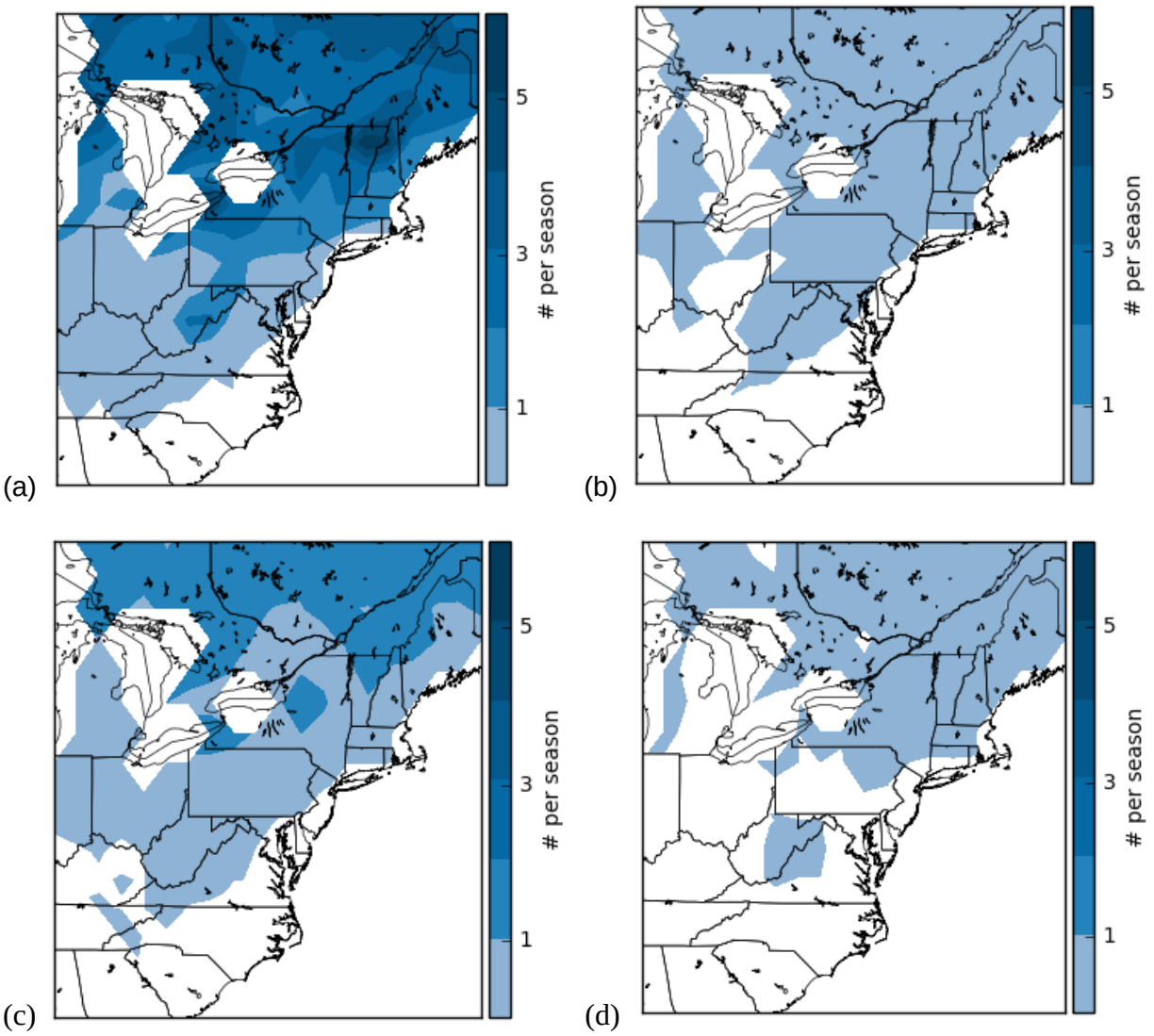

Figure 2.4. Number of ROS events per season for autumn (SON) for (a) D1, (b) D2, (c) D3, and (d) D4.

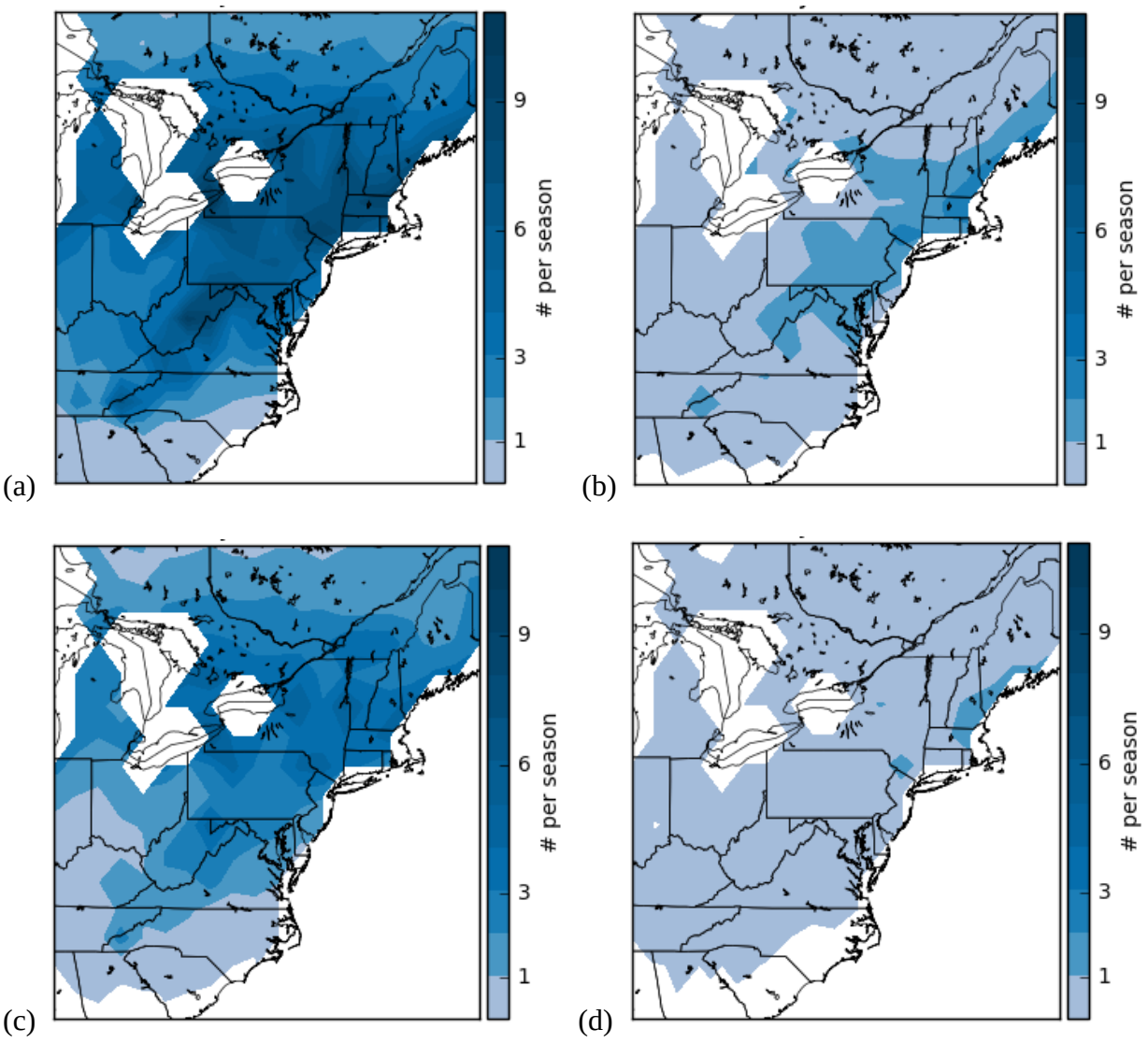

Figure 2.5. Number of ROS events per season for winter (DJF) for (a) D1, (b) D2, (c) D3, and (d) D4.

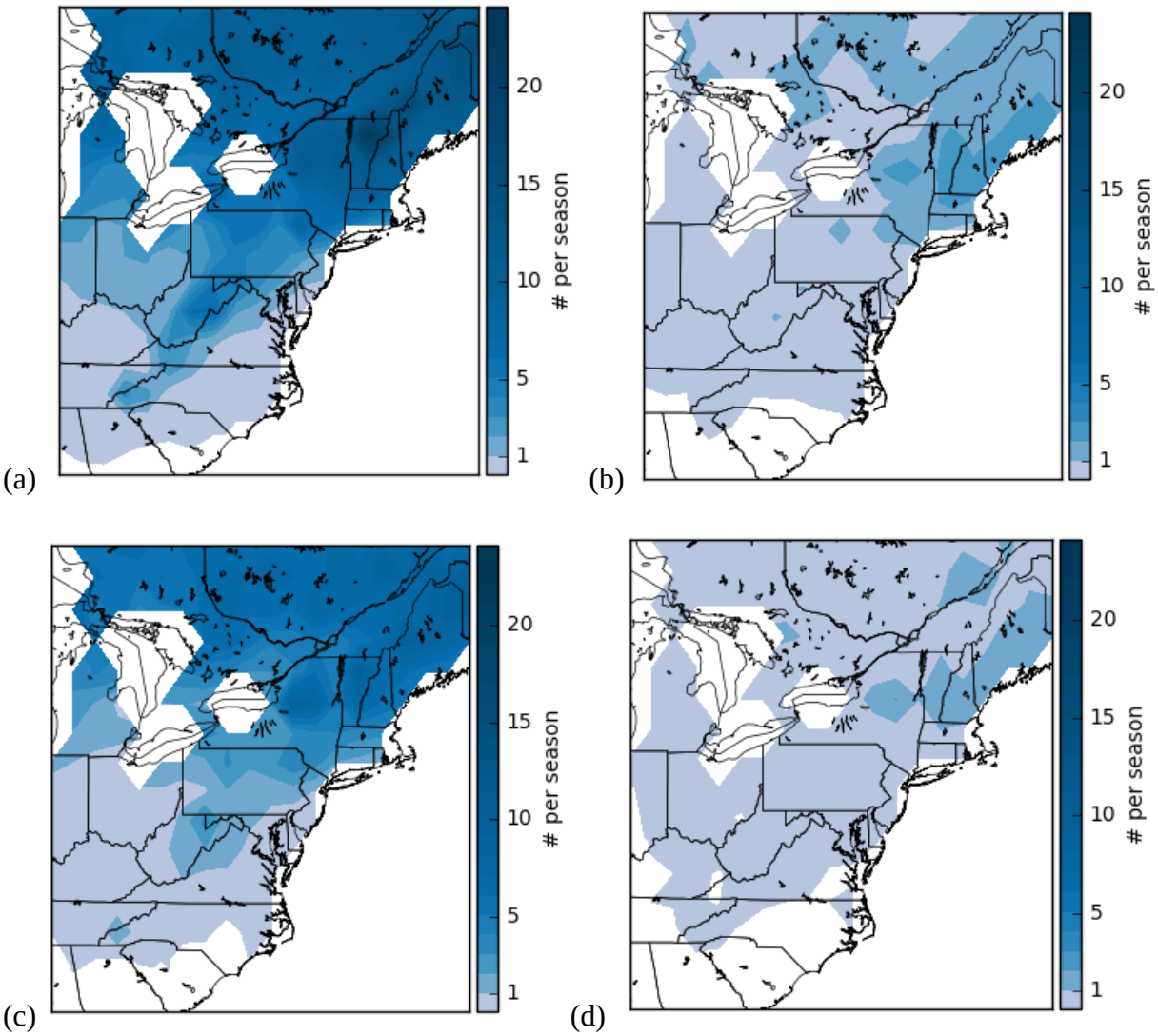

Figure 2.6. Number of ROS events per season for spring (MAM) for (a) D1, (b) D2, (c) D3, and (d) D4.

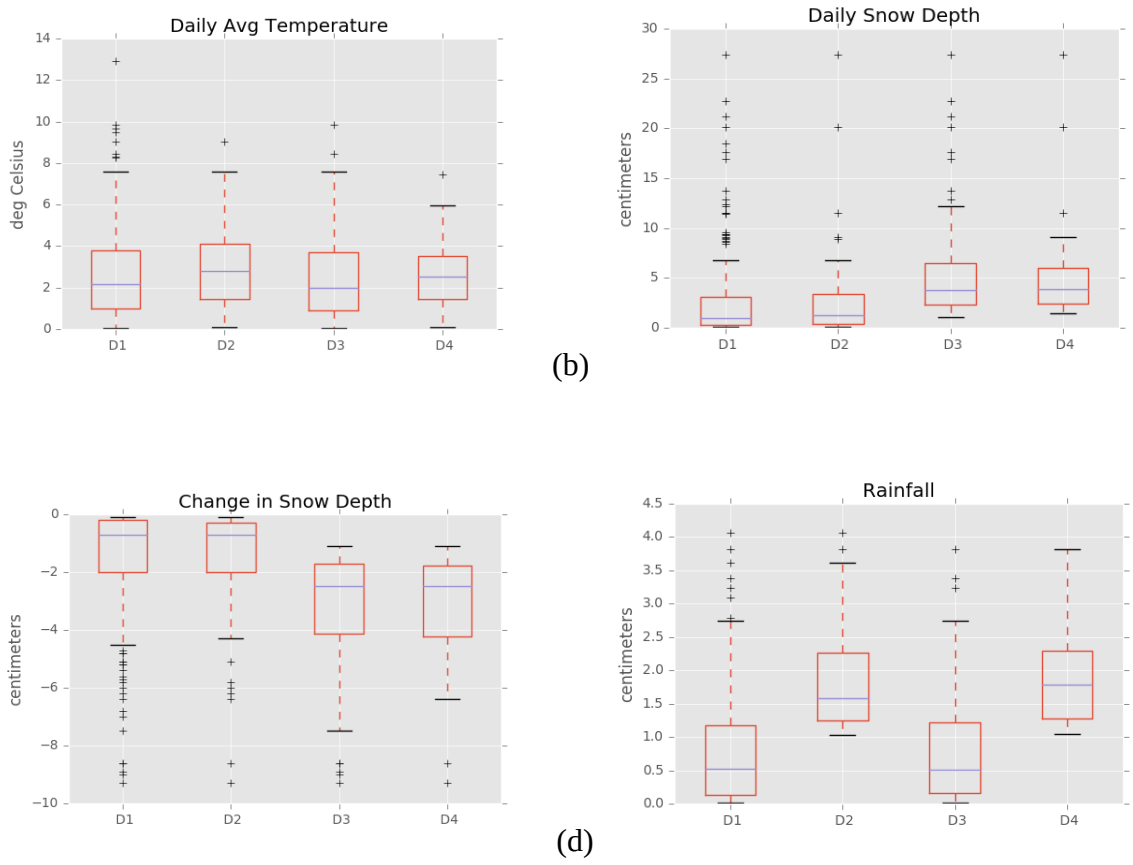

Figure 2.7. Average daily temperature in °C (a), daily snow depth in cm (b), change in snow depth in cm (c), and rainfall in cm (d) on ROS days at KPHL for each definition.

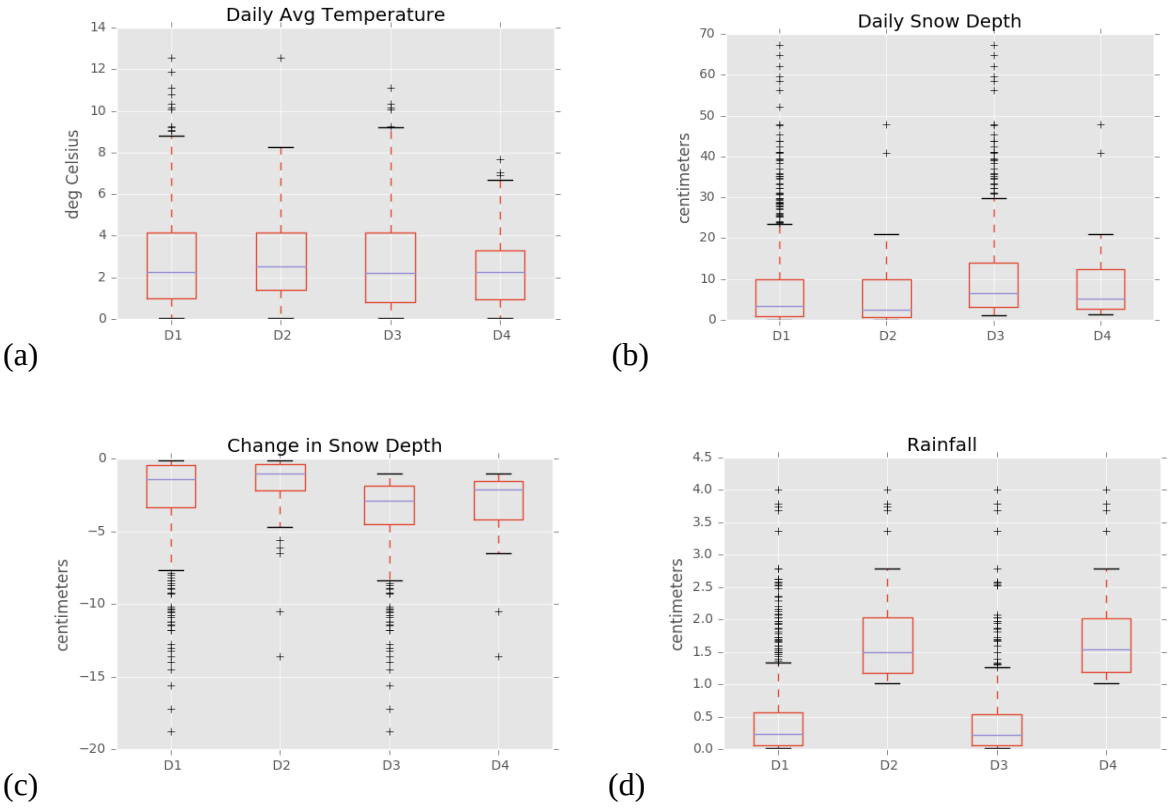

Figure 2.8. Average daily temperature in °C (a), daily snow depth in cm (b), change in snow depth in cm (c), and rainfall in cm (d) on ROS days at KBUF for each definition.

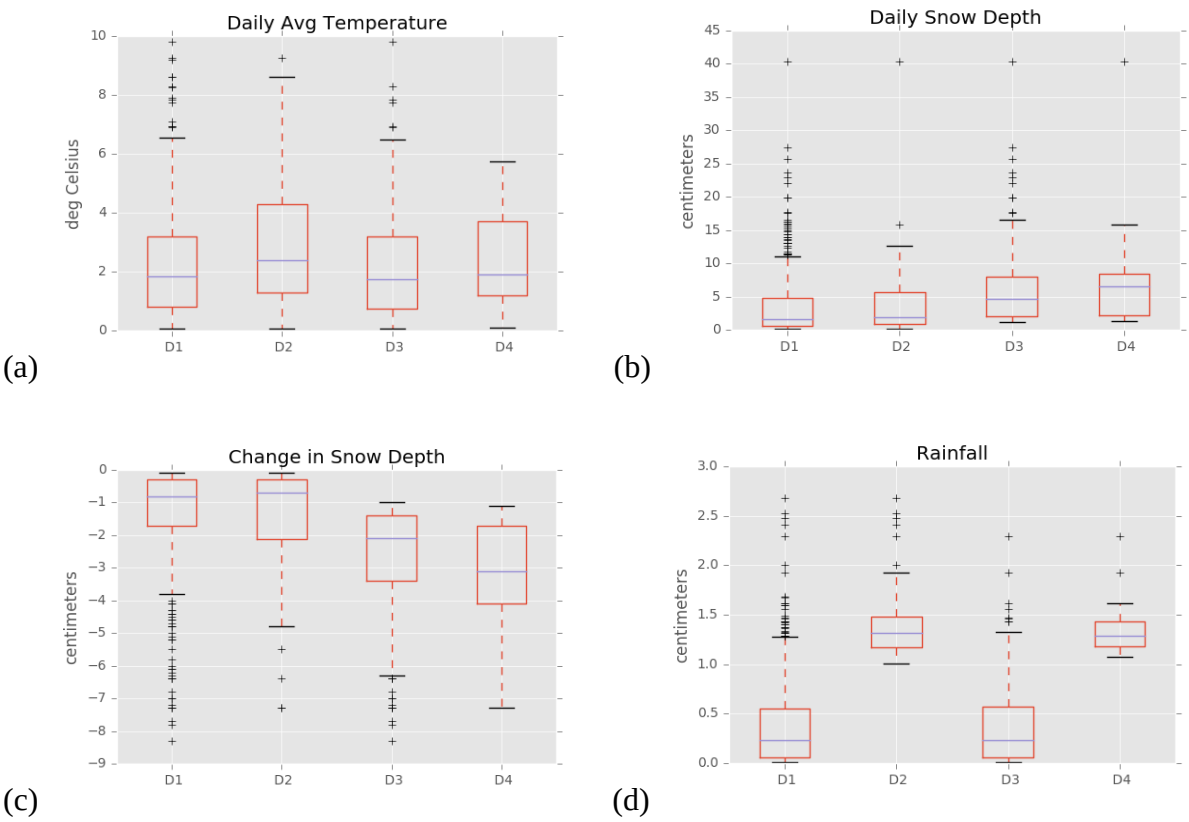

Figure 2.9. Average daily temperature in °C (a), daily snow depth in cm (b), change in snow depth in cm (c), and rainfall in cm (d) on ROS days at KFNT for each definition.

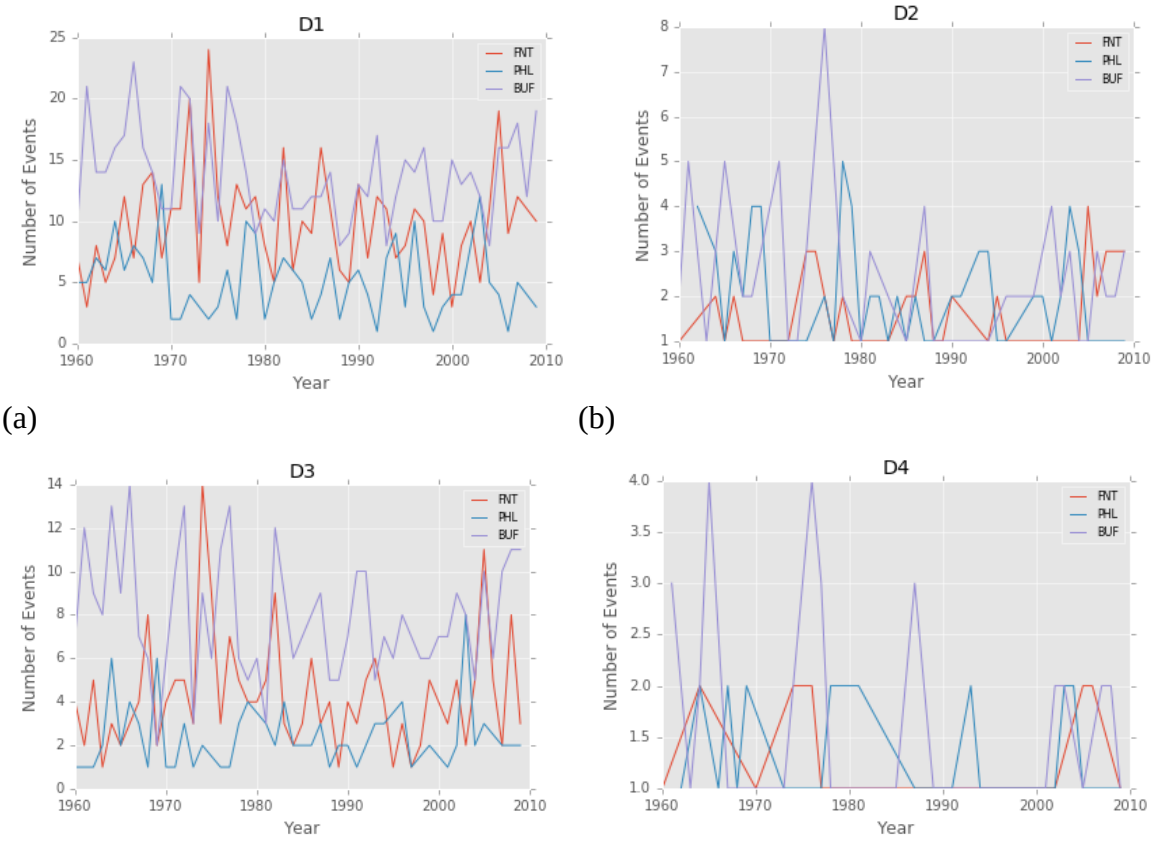

Figure 2.10. Time series of total counts per year for (a) Definition 1, (b) Definition 2, (c) Definition 3, and (d) Definition 4.

CHAPTER 3

ASSESSING THE IMPACT OF RAIN ON THE SURFACE ENERGY BUDGET OF A SNOWPACK IN THE MID-ATLANTIC UNITED STATES[2]

[2] Wachowicz, L. and T. Mote. To be submitted to *International Journal of Climatology*

Abstract

Rapid melting of a snowpack from rainfall has the potential to cause devastating floods, as the rain combined with warm, moist air can enhance the physical processes driving snowmelt. As differences in the magnitude of meteorological variables are largely driven by atmospheric circulation, limited research has looked at establishing a link between atmospheric circulation and the surface energy budget (SEB), particularly during rain-enhanced melt. Therefore, by using a synoptic classification scheme and a one-dimensional snowpack model, surface energy fluxes are established for primary modes of synoptic-scale circulation associated with rain-on-snow (ROS) in the mid-Atlantic region of the United States. In addition, a sensitivity analysis is conducted using the snowpack model, including and excluding precipitation.

Results show that ROS events are frequently associated with synoptic-scale circulation patterns conducive to stronger moisture transport into the mid-Atlantic region. When considering the link between atmospheric circulation and SEB, some variation in the SEB occurs between synoptic types where cooler, drier types are dominated by net shortwave radiation, and warmer types are driven by sensible heat fluxes. Additionally, much variation in magnitudes of SEB fluxes within synoptic types exists due to the effect of rainfall on the surface albedo of the snowpack. The presence of rainfall tends to play a role in changes of net shortwave radiation and significant changes in ground heat fluxes, particularly in instances when ROS is categorized under warm, moist synoptic types associated with strong moisture transport. Overall, this paper provides a first look into both establishing a connection between atmospheric circulation and ROS, and assessing the importance of rainfall during these events.

Key Words: Rain on snow, Surface energy budget, Synoptic climatology, Snowmelt

3.1 Introduction

Parts of the mid-Atlantic region of the United States, particularly those in higher elevations and higher latitudes, are subjected to large amounts of snowfall during its winter months. In areas where seasonal snow cover is present, the loss (ablation) of this snow cover depends on a variety of processes typically driven by air temperature and other factors such as wind and precipitation, which may enhance ablation. A subset of ablation events, known as "rain-on-snow" (ROS), are events where rain falls on an existing snowpack, enhancing ablation rates and potentially producing damaging flooding. Though infrequent, these ROS can lead to loss of life especially in areas where topography can enhance runoff, such as mountainous areas (Leathers et al. 1998; Graybeal and Leathers 2006; Ashley and Ashley 2008).

Ablation of a snowpack, including that from ROS, is dependent on a combination of meteorological and hydrological components, which drive the surface energy budget (SEB) and in turn, drive the ablation process. Many studies of ROS neglect the heat flux due to rainfall into the snowpack, despite findings suggesting heat added by rainfall can be a significant component in the SEB (e.g., Mazurkiewicz et al. 2008; Garvelmann et al. 2014; Jennings and Jones 2015). Rain may contribute heat flux of similar magnitude to sensible and latent heat fluxes (Jennings and Jones 2015). Little research has been published examining the sensitivity of the SEB during ROS events in the eastern U.S., as most research has focused on the western U.S. (e.g. Mazurkiewicz et al. 2008 and Jennings and Jones 2015) as well as Germany (Garvelmann et al. 2014).

Moreover, links between synoptic-scale environments associated with ablation and SEB have been established (Leathers et al. 2004; Grundstein and Leathers 1999), but little work has been published on the synoptic environments specific to ROS events (e.g. Collins et al. 2014).

Sensible heat flux typically dominates the SEB during snow ablation in warm, moist air masses (Leathers et al. 2004) in the mid-Atlantic region of the eastern U.S. As this air mass type is typically found in the warm sector of a mid-latitude cyclone, large ablation events are common when a snowpack is present preceding the passage of a cyclone (Grundstein and Leathers 1999).

Enhanced moisture transport within the warm sector of a mid-latitude cyclone can provide additional moisture and low-level winds as well as excess precipitation; the interaction of this feature with topography can potentially cause ROS events (Rössler et al. 2014; Guan et al. 2016). Furthermore, a comparison of two ROS events in the mid-Atlantic suggests that the duration of high winds and warm, moist air advection increases turbulent fluxes (Kroczynski 2004), aiding in snowpack ripening and thus contributing to the hydrologic consequences of an event. Therefore, the role of synoptic-scale circulation patterns in the SEB should be examined for ROS events. The aim of this paper is to 1) establish a link between synoptic-scale circulation and the surface energy budget during ROS, and 2) assess the sensitivity of the surface energy budget from rain during these events within the mid-Atlantic region of the U.S.

3.2 Data and Methodology

3.2.1 Identification of ROS events

Philadelphia, PA is centrally located within the mid-Atlantic region and in relatively close proximity (~ 280 km) to sites chosen in previous ablation studies (e.g., Leathers et al. 2004; Leathers et al. 1998). In addition to being a major city, Philadelphia is located between the east coast of the U.S. and the Appalachian Mountains, which may allow for interactions between the atmosphere and local topography to cause potentially devastating snowmelt-induced flooding in highly populated area.

ROS events are identified for a 1° x 1° grid cell containing Philadelphia using the Daily Gridded North American Snow, Temperature, and Precipitation Dataset (Kluver et al 2016; Dyer and Mote 2006). This dataset contains daily interpolated values of maximum and minimum temperatures (°C), precipitation (mm), snowfall (mm), and snow depth (m) from 1960 through 2009. A day with daily average temperatures greater than 0 °C, rainfall > 1 cm, and any decrease in snow depth (< 0 cm) in the next 24-hours is considered a "ROS date." The ROS dates used, which meet the rainfall and snow depth thresholds, are those identified in Wachowicz and Mote (in preparation); in addition these particular set of thresholds yielded a larger sample of events than those with stricter snow depth thresholds combined with a strict rainfall threshold.

3.2.2 Synoptic Typing

Using the Temporal Synoptic Index (TSI; Kalkstein and Corrigan 1986), common synoptic-scale circulation patterns are extracted for KPHL. The TSI is a synoptic climatological approach, utilizing both clustering and principal component analysis (PCA) to extract primary modes of synoptic-scale circulation. This index categorizes different air masses based on a variety of meteorological variables (e.g., air pressure, temperature, wind speed components, and cloud cover) at four different times each day for a given location and accounts for seasonal differences. Furthermore, while the TSI was initially used in applied climatological studies, particularly those relating to air pollution (e.g., Kalkstein and Corrigan 1986), recent work relating to ablation and snowfall has used this approach (e.g., Suriano and Leathers 2017a, 2017b).

A synoptic calendar for KPHL was produced using daily meteorological measurements (i.e., air pressure, temperature, wind speed components, and cloud cover) collected 4 times daily (0900Z, 1500Z, 2100Z, 0300Z) during 1948 – 2015, generated using a TSI procedure similar to

Suriano and Leathers (2017a, 2017b), which associates each day with a synoptic type. The synoptic calendar as well as qualitative descriptions of each synoptic type for KPHL were obtained from the Rutgers Global Snow Lab.

3.2.3 MERRA-2 dataset

The Modern-Era Retrospective analysis for Research and Applications (MERRA-2; Gelaro et al. 2017) reanalysis dataset is used in making synoptic composites of sea level pressure, 500 hPa height, 850 hPa moisture and wind fields, and estimated precipitation. This reanalysis dataset is available at a 0.625° by 0.5° spatial resolution and comprises of 42 standard pressure levels (or 72 model layers). Daily averages for the composites are made 00Z – 00Z for identified ROS dates occurring between 1980 – 2009, as MERRA-2 is available beginning 1980.

3.2.4 Snow energy and mass balance model

The SNow THERMal model (SNTHERM; Jordan 1991) is used to assess the sensitivity of the surface energy budget from rain on the snowpack during ROS events. To provide estimates of the SEB, SNTHERM models seasonal snow cover through simulating heat and mass transfers through the snowpack with the atmosphere and ground to account for accumulation, melt as well as compaction (Jordan 1991). SNTHERM has demonstrated the potential to accurately model SWE (Grundstein et al. 2002) as well as snow depth and radiative fluxes (Grundstein and Leathers 1999), resulting in relatively small model errors and high agreement between modeled and measured variables. Output from SNTHERM consists of energy budget terms (W m^{-2}) as well as various snow-related variables, including snow depth (m), snow water equivalent (cm), and melt flux (kg m^{-2}).

Hourly meteorological station data (i.e., temperature, relative humidity, wind speed, precipitation, and cloud cover) from Philadelphia International Airport (KPHL) are used to drive

SNTHERM. In the event hourly data are missing, linear interpolation is used to fill in the missing hour for temperature, relative humidity, and wind speed. Missing precipitation data is considered to be 0. Missing cloud cover data is estimated using the suggested convective scheme from Grundstein et al. (2002). Instead of using observed snow depth, SNTHERM simulations are conducted for an 8-day period with an initial snow depth of 1.4 m, per Leathers et al. (2004) to allow for a 3-day spin-up time is to equilibrate the model. This ensures snow depth is approximately 1 m 24-hours before a ROS day starts for each event such that the snowpack does not melt over the duration of the event. As the use of SMTHERM was for sensitivity analysis, not to reproduce snowpack conditions on any given day, a nearly uniform initial snow depth across events allows for comparison of the impact of rainfall on ablation between different synoptic types.

3.3 Results

3.3.1 Meteorological characteristics associated with common ROS synoptic types

ROS dates between 1980 and 2009 were extracted from the KPHL synoptic calendar, where frequencies of synoptic types were computed on ROS days to ascertain the common types associated with ROS (Table 3.1). The synoptic calendar indexes each day with its synoptic type and average meteorological characteristics; the names of the synoptic types are subjective and were adopted from the names provided by Zachary Suriano (personal communication) and available through the Rutgers University Global Snow Lab.

Of the four synoptic types most frequently associated with winter (DJF) ROS events, the Great Lakes Low (TSI 1031) is the most frequent type, with 193 days total during DJF between 1980 and 2009. The Weak Carolinas Low (TSI 1004) is the least common, only occurring on 79 total days between 1980 and 2009. Both the Mid-Atlantic Coastal Low (TSI 1032) and New

England Low (TSI 1011) nearly equally as common, occurring on 108 and 104 total days, respectively.

ROS is most commonly associated with Mid-Atlantic Coastal Lows (1032), where five of the 108 total days experiencing this synoptic type (or 4.6% of days) during the DJF season meet ROS criteria. Furthermore, four total ROS events occur on days in which a Weak Carolinas Low (1004), New England Low (1011), or Great Lakes Low (1031) is present. Of these four synoptic types, although the Great Lakes Low is the most common circulation pattern, ROS is only present on 2.1% of these days. Additionally, more than 5% of days experiencing a Weak Carolinas Low (1004) are considered ROS. Furthermore, ROS is present on nearly 4% or more of the days with a Mid-Atlantic Coastal Low (1032) or New England Low (1011).

The average meteorological conditions for each synoptic type at KPHL from 1948 – 2015 is shown in Table 3.2 and is compared to the average meteorological conditions occurring during the identified ROS days from 1980 – 2009. Generally, ROS events are associated with surface cyclones. All days during 1948–2015 with a Mid-Atlantic Coastal Low (1032) were generally characterized as being colder compared to other common synoptic types, with temperatures near or below 0°C, low dew point temperatures, northeast and/or northwest flow, and cloudy conditions. In general, days with a Great Lakes Low (1031) were characterized by above-freezing temperatures, slowly become much warmer (near 9°C) during the day. Dew point temperatures also tended to increase during the day to +2–3°C. Additionally, southwesterly flow is common, and this type typically has the lowest cloud cover of the four types. The New England Low (1011) remains within +4–5°C at its warmest period, with dew point temperatures at or as much as 6°C below freezing toward the end of the day. This type is characterized with high cloud cover and more westerly flow. Lastly, the Weak Carolinas Low (1004) is generally a

warmer synoptic type, with temperatures 3°C or more above freezing and dew point temperatures near +2°C or higher. Moreover, northeasterly wind is typically common with nearly overcast conditions throughout the day.

Figures 3.1, 3.2, and 3.3 show composites of sea level pressure and 500 hPa heights (Figure 3.1), precipitable water vapor and 850 hPa winds (Figure 3.2), and rainfall rates (Figure 3.3) between the different synoptic types for ROS days. ROS events associated with the Mid-Atlantic Coastal Low (1032) indicated a weak low pressure system along the coast of the mid-Atlantic ahead of a weak upper level trough (Figure 3.1a). The weak flow suggests little temperature advection into the area during this time, with near-freezing temperatures throughout the period in which ROS occurs (Table 3.2). Though precipitable water vapor (Figure 3.2a) values of 15–20 mm were located nearby, rainfall rates remained rather low, around 0.1 mm hr^{-1} (Figure 3.3a).

More generally, ROS events resulting from a Weak Carolinas Low (1004) tended to be associated with increasing temperatures and higher humidity (Table 3.2). A strong pressure gradient ahead of a surface low (Figure 3.1b) with moderate winds of about 15 m s^{-1} at the 850 hPa level contributed to temperature and moisture advection (Figure 3.2b). As a result, average precipitation rates remained rather high (over 1 mm hr^{-1}), partly due to shorter-lived but higher precipitation rates during the ROS period (Figure 3.3b). Given the strong moisture transport into the region shown by the precipitable water values nearing 30 mm and stronger winds at 850 hPa, it is likely that localized heavy precipitation occurred as a result of the interaction of this plume with local topography.

Similar to the Weak Carolinas Low, the New England Low (1011) also experienced higher precipitation rates on average (Figure 3.3c) nearing 0.5 mm hr^{-1}, not unexpected given the

distribution of precipitable water vapor over the mid-Atlantic region (Figure 3.2c). Though a plume of moisture was advected into the region, it was generally weaker than what is associated with the Weak Carolinas Low (1004). However, like the Weak Carolinas Low, the interaction of this plume with local topography could have played a role in the distribution of precipitation. The position of a surface high over the Atlantic with a trough present over the northeastern portion of the U.S. (Figure 3.1c) was conducive to weak temperature advection as temperatures remain 4–5°C above freezing, particularly earlier in the day (Table 3.2). The average temperature later in the day during events of this type tended to be lower when compared to the Weak Carolinas Low (Table 3.2).

ROS events associated with the Great Lakes Low (1031) were the result of a strong low located over the Great Lakes region with a high over the Atlantic (Figure 3.1d). Temperatures throughout the period remained relatively high, +1–5 °C, through the duration of the day (Table 3.2). Precipitable water vapor values near 20 – 25 mm were present in the region with higher amounts located off the coastline (Figure 3.2d), associated with higher precipitation rates near 0.5 – 1 mm hr^{-1} (Figure 3.3d). However, less moisture advection into the region was present during this period compared to the Weak Carolinas Low (1004) despite wind speeds near 15 m s^{-1} at the 850 hPa level (Figure 3.2d). The plume of moisture advected into the region was less pronounced with lower precipitable water values than that of the Weak Carolinas Low.

3.3.2 Energy Budget during ROS

Average modeled fluxes occurring during the ROS events are shown in Table 3.3, which shows variation within each synoptic type as well as the variation between the four common synoptic types. The most common synoptic type (Mid-Atlantic Coastal Low 1032) had more net shortwave and sensible heat flux added heat into the snowpack on average across all events of

this type. Given the above-freezing air temperatures and lower precipitable water vapor values, this is intuitive. A negative net longwave radiation (-10 W m^{-2}) and latent heat flux (-7 W m^{-2}) indicate precipitation likely played a smaller role in the melt process when compared to temperature, wind, and cloud cover by acting to produce condensation, as the net heat into the snowpack for this synoptic type was roughly 17 W m^{-2} on average.

The Weak Carolinas Low (1004) impact on ROS was dominated by heat input from net shortwave radiation and sensible heat flux, with an average of nearly 13 W m^{-2} of energy being added to the snowpack from both components. As ROS events of this synoptic type were dominated by higher temperatures, higher humidity, and higher precipitation rates, it is likely that sensible played a dominant role in the heating of the snowpack, as net longwave radiation, latent, and ground heat fluxes remained low or near-zero. Furthermore, net longwave radiation tends to be a source of heat with 8.3 W m^{-2} added into the snowpack from the cloudy and moist conditions. Given the similarity between the Weak Carolinas Low (1004) and New England Low (1011), similar energy fluxes are present within the New England Low with the exception of higher net longwave radiation values, about 8 W m^{-2} versus 2.5 W m^{-2} seen in the Weak Carolinas Low. This is likely due to the differences in cloud cover between the Weak Carolinas Low (1004) and New England Low (1011), which is shown in Table 3.2.

Lastly, above-freezing temperatures in combination with higher wind speeds play a large role in the energy budget during ROS events of the Great Lakes Low (1031), with high sensible heat fluxes near 17 W m^{-2} and negative latent heat fluxes near -4 W m^{-2}. This synoptic type also exhibits high relative humidity as well as higher precipitation rates, where high relative humidity may be producing condensation on the surface of the snowpack, particularly during instances of rainfall.

While the difference in the radiative, sensible and latent heat fluxes among the synoptic types is modest, it is important to note that these differences are in the mean values. A single-factor "Analysis of Variance" (ANOVA) was employed for each type of energy flux (i.e., net shortwave, net longwave, sensible, latent, and ground heat fluxes). As ANOVA is widely used for testing differences in the statistical mean between groups, results can show whether the distribution of mean fluxes differ significantly ($p \leq 0.05$) across each synoptic type (i.e., Mid-Atlantic Coastal Low, Weak Carolinas Low, New England Low, and Great Lakes Low). For a given flux (e.g., net radiation) the daily fluxes from individual events (from Table 3.3) within the synoptic type were compared across synoptic types to discern any significant differences. These results are summarized in Table 3.4. Results indicate that for each type of flux, there is no significant change in distribution of the flux across each synoptic type ($p > 0.05$). Given this outcome, it is possible that more extreme events falling under the different synoptic types drive the changes in magnitudes of the different fluxes during ROS events, although the average conditions associated with each type of event do not vary as much.

3.3.3 Role of precipitation in ROS

SNTHERM simulations in which precipitation (both rain and snow) was excluded over the 8-day period were used to test the influence of rainfall on the SEB. Figure 3.4 shows a comparison in the modeled fluxes (K_{net}, L_{net}, Sensible, Latent, and Ground fluxes) for the ROS and no-precipitation events. This comparison of the SEB terms on ROS days suggests the presence of precipitation appears to have some influence on the energy budget (Figure 3.4). More specifically, the presence of precipitation appears to change the impact of both net shortwave radiation and ground heat flux for all common synoptic types, whereas precipitation played a minor role in the amount of net longwave radiation, as well as sensible and latent heat fluxes.

The large differences in the impact of ground heat flux on the SEB between scenarios – despite being relatively small in magnitude when compared to the other fluxes – show that precipitation may have reduced the temperature gradient through the release of latent heat by condensation at the surface and between the soil and the snow by warming the snowpack as meltwater percolates through the snowpack. This occurred mostly in instances where a Mid-Atlantic Low (1032) or Great Lakes Low (1031) were present. On the contrary, the lack of precipitation allowed the snowpack to maintain a larger temperature gradient and therefore allowed more heat transfer from the ground resulting in more energy available for melt. This difference was much greater for the Weak Carolinas Low (1004) and Great Lakes Low (1031), both of which had higher rainfall rates.

To test whether the differences seen between the rain and no-precipitation scenarios are significantly different for each type of flux, a paired two sample Student's t-test was conducted. The results of the t-test with alpha ≤ 0.05 indicate the only significant differences between ROS and no-precipitation scenarios for the Weak Carolinas Low (1004) for a 2-tail test (Table 3.6; $p < 0.05$). Furthermore, the difference in ground heat flux between scenarios is likewise considered significant for a 1-tail Student's t-test (Table 3.7; p-value ≤ 0.05) for the Great Lakes Low (1031). Little variation in ground heat flux is present between precipitation scenarios for the New England Low (1011), despite the higher temperatures and inferred warmer precipitation producing condensation at the surface of the snowpack with rainfall, which would act to ripen the snowpack.

In most cases changes in net shortwave radiation between precipitation scenarios, albedo (not shown) was much higher when precipitation (both rain and any additional snow) was not present. This is because the rain acts to lower the albedo of the surface of the snowpack,

therefore allowing more shortwave radiation to be absorbed. More net heat went into the snowpack as a result of precipitation in most cases (Table 3.3) compared to no precipitation (Table 3.5), particularly for the Mid-Atlantic Coastal Low (1032). Despite the changes in magnitude of K_{net} between scenarios, these differences were not significant based on a 2-tail Student's t-test (Table 3.8).

Moreover, the magnitudes of turbulent fluxes (sensible and latent) tended to vary slightly ($0.1 – 0.2$ W m^{-2}) as a result of precipitation, depending on the synoptic type. Although small, sensible heat flux differences particularly for the Great Lakes Low (1031) as well as latent heat flux differences from the Great Lakes Low and mid-Atlantic Coastal Low (1032), suggest the role of precipitation in ROS may vary more on an event-by-event basis than on synoptic type.

Lastly, time series (Figures 3.5 to 3.9) showing modeled flux components between the rain and no-precipitation scenarios show some variability in terms of magnitudes of turbulent fluxes the day after ROS for these two events. In most cases, while precipitation did not appear to have a strong impact on the SEB during ROS, the largest differences in energy budget fluxes tended to occur after the 24-hour ROS period, suggesting that any heat added by rainfall produced a lag in the snowpack melting process. This is particularly true for K_{net} for the Mid-Atlantic Coastal Low (1032) likely due to the changes in albedo of the snowpack (Figure 3.5). Changes in cloud cover (e.g., type of clouds and cloud cover fraction) are the likely cause in change in L_{net} the following day for the New England Low (1011) and Mid-Atlantic Coastal Low (Figure 3.6), Differences in magnitudes of sensible and latent heat fluxes are present in the New England Low likely because of the presence of precipitation during ROS acted to ripen the snowpack and increased its sensitivity to temperature, moisture, and wind into the following day (Figures 3.7 and 3.8, respectively). Lastly, Figure 3.9 shows a difference in amount of ground

heat flux for each event, regardless of synoptic type indicating ground heat flux is typically larger when precipitation is not present. This may be the result of a denser snowpack after the initial rainfall, therefore weakening the impact of ground heat on the snowpack.

The timing of the lag, as well as magnitudes of fluxes changing after the ROS period, also varied by individual event more so than by synoptic type. This also suggests consideration of the transitions between synoptic types could play a role in the snowpack ripening process as well as affecting the timing of precipitation, which may act to enhance the ripening process on a more case-by-case basis.

3.4 Conclusion

Using a 1° x 1° gridded data set, rain-on-snow events in which at least 1 cm of rainfall was measured within the cell and a measureable amount in loss in snow depth (i.e. > 0 cm) were identified for Philadelphia. Common modes of synoptic scale circulation occurring on ROS days were identified and an average energy budget during these events was produced for each synoptic type using a one-dimensional surface energy budget and mass balance model. Model simulations in which precipitation was excluded were used to produce a comparison to test the influence of precipitation on the energy budget. The main findings of this paper are as follows:

1. ROS events were commonly associated with surface cyclone passages. Each type of synoptic-scale circulation has differing meteorological characteristics (temperature, relative humidity, wind speed, and precipitation rates) during periods of ROS in the winter months. Synoptic types (e.g., the Mid-Atlantic Coastal Low) consisting of slightly above-freezing temperatures and relatively drier air were most frequently present in Philadelphia and most commonly associated with ROS in this area. In addition, a less-common Weak Carolinas Low type tended to have a higher percent of ROS days, as it

was associated with higher temperatures and larger amounts of moisture advection. However, warmer and/or more moist conditions occurring with other common synoptic types (i.e., Great Lakes Low and New England Low) were often conducive to ROS.

2. Depending on the synoptic type, different types of fluxes in the SEB tended to dominate. Net shortwave radiation tended to play a larger role in more of the events with cooler, drier synoptic types (e.g., Mid-Atlantic Coastal Low), while sensible heat played a large role in the Great Lakes Low synoptic type, which has higher temperatures. However, the magnitude of each flux varies within each synoptic type, which may suggest other factors (e.g., timing of precipitation, precipitation amount, etc.) playing into the ripening process of the snowpack. The variation of meteorological characteristics within synoptic types may further enhance or repress the magnitude of certain fluxes.
3. While the presence of precipitation (mostly rain) had little influence in differentiating synoptic types, precipitation can play a larger role on an event-by-event basis. In most cases, the presence of precipitation acted to decrease the surface albedo of the snowpack and allowed for more absorption of shortwave radiation. These cases generally had a higher net heat flux added into the snowpack than their no-precipitation counterparts. Furthermore, particularly for the Great Lakes Low and Weak Carolinas Low, the presence of rain significantly affected the ground heat flux. A larger sample of events within each synoptic type may help alleviate the uncertainty with the link between synoptic-scale circulation and SEB.
4. In addition, variation in the SEB resulting from rain was rather small during the period in which ROS is happening. However, larger differences between precipitation and no-precipitation scenarios tended to result in the day following the main ROS event, likely

due to snowpack processes requiring a lag in order to start melting. Mechanisms driving the timing of the melt (e.g., cold content of snowpack, transitions between synoptic types, etc.) were not considered in this paper, and should be considered with future work.

In conclusion, this paper provides an initial investigation into the relationship between atmospheric moisture content associated with synoptic-scale atmospheric circulation and the sensitivity of the surface energy budget of the snowpack during rain-on-snow. Results indicate an apparent connection between the two, with this connection potentially varying more on an event-by-event basis than based on synoptic-scale circulation. Additionally, the role of rainfall during these events is addressed and suggests the sensitivity of the snowpack from rainfall may also be influenced by this connection. Furthermore, this paper contributes to broadening current understanding of ROS events, especially in the mid-Atlantic region with limited past ROS research.

3.5 References

Ashley, S. T. and W. S. Ashley, 2008: The storm morphology of deadly flooding events in the United States, *Int. J. Climatol*., **28**, 493–503, doi:10.1002/joc.1554.

Collins, M. J., J. P. Kirk, J. Pettit, A. T. DeGaetano, M. S. McCown, T. C. Peterson, T. N. Means, and X. Zhang, 2014: Annual floods in New England (USA) and Atlantic Canada: synoptic climatology and generating mechanisms, *Phys. Geogr.,* **35**, 195-219.

Dyer, J. L., and T. L. Mote, 2006: Spatial variability and trends in observed snow depth over North America, *Geophys. Res. Lett*., **33**, L16503, doi:10.1029/2006GL027258.

Garvelmann, J., S. Pohl, and M. Weiler, 2014: Variability of observed energy fluxes during rain-on-snow and clear sky snowmelt in a midlatitude mountain environment, *J. of Hydrometeor.,* **15**, 1220-1237.

Graybeal, D. Y., and D. J. Leathers, 2006: Snowmelt-related flood risk in Appalachia: first estimates from a historical snow climatology, *J. of Appl. Meteor. Climatol.,* **45**, 178-193.

Gelaro, R., W. McCarty, M. J. Suárez, R. Todling, A. Molod, L. Takacs, et al., 2017: The modern-era retrospective analysis for research and applications, version 2 (MERRA-2), *J. Clim.*, **30**, 5419-5454.

Grundstein, A. J., and D. J. Leathers, 1999: A spatial analysis of snow-surface energy exchanges over the northern Great Plains of the United States in relation to synoptic scale forcing mechanisms, *Int. J. Climatol.,* **19**, 489-511.

Grundstein, A., T. Mote, and D. Leathers, 2002: A hybrid climatology of snow water equivalent over the northern Great Plains of the United States, *Polar Geogr.*, **26**, 187-209.

Guan, B., D. E. Waliser, F. M. Ralph, E. J. Fetzer, and P. J. Neiman, 2016: Hydrometeorological Characteristics of Rain-on-Snow Events Associated with Atmospheric Rivers, *Geophys. Res. Lett.*, **43**, 2964-2973.

Jennings, K. and J. A. Jones, 2015: Precipitation‐snowmelt timing and snowmelt augmentation of large peak flow events, western Cascades, Oregon, *Water Resour. Res.*, **51**, 7649-7661.

Jordan, R., 1991: A one-dimensional temperature model for a snow cover: Technical documentation for SNTHERM.89. Special Report 91-16, 49 pp. [Available from U.S. Army Corps of Engineers, Cold Regions Research and Engineering Laboratory, Hanover, NH 03755.]

Kalkstein, L. S., and P. Corrigan, 1986: A synoptic climatological approach for geographical analysis: assessment of sulfur dioxide concentrations. *Ann. Assoc. Am. Geogr.* **76**, 381-395.

Kluver, D., T. Mote, D. Leathers, G. R. Henderson, W. Chan, and D. A. Robinson, 2016: Creation and validation of a comprehensive 1 by 1 daily gridded North American dataset for 1900–2009: snowfall. *J. Atmos. Oceanic Technol.*, **33**, 857-871.

Kroczynski, S., 2004: A comparison of two rain-on-snow events and the subsequent hydrologic responses in three small river basins in Central Pennsylvania, Eastern Region Technical Attachment, **4**, 1–21.

Leathers, D. J., D. Graybeal, T. Mote, A. Grundstein, and D. Robinson, 2004: The role of airmass types and surface energy fluxes in snow cover ablation in the central Appalachians, *J. of Appl. Meteor. Climatol.*, **43**, 1887-1899.

Leathers, D. J., D. R. Kluck, and S. Kroczynski, 1998: The severe flooding event of January 1996 across north-central Pennsylvania, *Bull. Am. Meteor. Soc.*, **79**, 785.

Mazurkiewicz, A. B., D. G. Callery, and J. J. McDonnell, 2008: Assessing the controls of the snow energy balance and water available for runoff in a rain-on-snow environment, *J..Hydrol.*, **354**, 1-14.

Rössler, O., P. Froidevaux, U. Börst, R. Rickli, O. Martius, and R. Weingartner, 2014: Retrospective analysis of a nonforecasted rain-on-snow flood in the Alps–a matter of model limitations or unpredictable nature, *Hydrol. Earth Syst. Sci*, **18**, 2265-2285.

Suriano, Z. J., and D. J. Leathers, 2017a: Synoptically classified lake-effect snowfall trends to the lee of Lakes Erie and Ontario, *Clim. Res.*, **74,** 1-13, doi: 10.3354/cr01480.

Suriano, Z. J. and D. J. Leathers, 2017b: Synoptic climatology of lake-effect snowfall condition in the eastern Great Lakes region. *Int. J. Climatol.,* **37**, 4377-4389, doi: 10.1002/joc.5093.

Wachowicz, L. J., and T. L. Mote, 2017: Establishing a rain on snow climatology in the eastern United States. In preparation.

3.6 Tables and Figures

Table 3.1. Common TSI synoptic type and descriptions associated with ROS dates from 1980 – 2009 at KPHL; total number of days of identified under the given synoptic type and percentage of the total in which ROS occurred are included.

Synoptic Type	Description	Number of Days	Percent of ROS days	ROS Dates
1032	Mid-Atlantic Coastal Low	108	4.6	19820219
				19850202
				19870223
				20021211
				20050221
1004	Weak Carolinas Low	78	5.1	19860218
				20030222
				20031214
				20091226
1011	New England Low	104	3.8	19880118
				19900108
				19960119
				20000219
1031	Great Lakes Low	193	2.1	19820203
				19830207
				19940128
				20040203

Table 3.2. Average meteorological characteristics for each synoptic type from the TSI synoptic calendar and number of events (N) for 1949–2015 as well as the subset of ROS dates analyzed in this paper during 1980–2009; variables included are air temperature (T, ºC.), dew point (T_d, ºC), sea level pressure (SLP, hPa), u and v wind components (u, v, m s^{-1}), and cloud cover fraction (CC). Precipitation measurements are not included.

		1948–2015				**1980–2009**			
Time		**1032**	**1004**	**1011**	**1031**	**1032**	**1004**	**1011**	**1031**
	N	283	166	248	407	5	4	4	4
9UTC	T	-0.8	3.6	3.3	2	0.7	2.2	4.7	1
day+0	T_d	-4.5	1.2	0.3	-0.9	-2.5	-0.3	4.3	-0.3
	SLP	1010.8	1014.2	1010.8	1014.2	1014.9	1017.9	1013.2	1018.2
	u	-1.8	-3.9	1.2	0.1	-4	-3	-0.8	-2.4
	v	-3.1	-2.8	1.5	-0.2	-2.8	-2	2.2	-2.8
	CC	9.3	9.7	9.5	6	10	10	10	10
15UTC	T	-0.3	4.6	4.5	5.5	1.2	3.4	5.8	4.6
day+0	T_d	-4.2	2.3	0.3	1.3	-0.8	2.4	5	3.2
	SLP	1009.4	1012.6	1010.7	1012.9	1014.3	1014.4	1011.2	1013.8
	u	-1.3	-4.8	3.2	0.6	-1.6	-5.4	-1.3	-2.7
	v	-3.9	-3.3	0.1	1	-2.7	-3	2.9	0.7
	CC	9.7	9.8	9.3	7.4	10	10	10	10
21UTC	T	0.6	5.5	4.9	9.4	3	5.7	4.5	5.4
day+0	T_d	-4.3	3.4	-2.7	3.2	0	5	3.6	4.6
	SLP	1007	1008.3	1010.4	1007.7	1012.2	1007	1008.9	1008.4
	u	0.7	-3.7	4.9	1.8	1.6	-4.3	3.8	2.9
	v	-4.6	-3.3	-3	2.8	-3.1	-1.9	-3.3	0.4
	CC	9.4	9.9	8.6	8	10	10	10	10
3UTC	T	-1.5	4.4	0.7	6.7	1.6	5.7	-0.1	4.1
day+1	T_d	-6.3	2.4	-6.4	3.1	-1.8	5.1	-1.5	2.2
	SLP	1009	1007.5	1015	1007.2	1014	1005.3	1016.5	1010.6
	u	1.8	-1.7	3.9	2.4	0.9	0.4	5.4	3.7
	v	-4.2	-3.2	-3.6	1.9	-2.8	-2.2	-2.9	0.8
	CC	7.8	9.5	5.7	7.6	7.6	10	5	8.1

Table 3.3. Average daily flux components (W m^{-2}) and albedo (a) as well as modeled temperature (T, °C), relative humidity (RH, %) and wind speed (WS, m s^{-1}) for the common synoptic types associated with ROS for each event as well as an average for each synoptic type.

	Date	K_{net}	K_d	K_u	a	L_{net}	L_d	L_u	H	LE	G	T	RH	WS	NET
1004	19860218	21.6	96.1	74.5	0.3	-1.7	313.7	315.5	6.2	0.2	0.7	2.9	95.0	3.8	26.9
	20030222	22.3	74.0	53.6	0.4	-3.2	312.2	315.5	5.2	0.2	-0.1	2.4	92.9	3.6	24.3
	20031214	6.5	70.4	63.9	0.3	-6.2	303.0	309.3	23.6	-0.3	-0.2	1.4	69.4	5.2	23.4
	20091226	4.1	41.4	37.3	0.3	21.0	337.2	315.5	16.4	1.2	0.8	7.5	96.5	6.4	43.5
	Average	13.6	70.5	57.3	0.3	2.5	316.5	314.0	12.8	0.3	0.3	3.5	88.5	4.8	29.5
1011	19880118	6.0	65.8	59.8	0.4	-0.4	314.0	314.4	7.3	0.1	1.5	3.2	87.7	2.9	14.4
	19900108	8.3	85.4	77.1	0.4	-9.6	302.2	312.1	2.3	-0.9	0.6	0.6	88.2	2.4	0.7
	19960119	6.4	67.1	60.7	0.4	49.0	366.1	315.5	30.0	3.7	0.9	13.2	92.7	8.8	90.0
	20000219	27.8	100.9	73.1	0.4	-5.7	309.6	315.5	3.4	0.1	-0.1	1.6	97.6	3.4	25.5
	Average	12.1	79.8	67.7	0.4	8.3	323.0	314.4	10.8	0.8	0.7	4.7	91.6	4.3	32.7
1031	19820203	5.7	60.6	54.9	0.4	0.7	316.1	315.4	21.7	-0.2	0.1	3.4	89.6	4.1	27.9
	19830207	18.7	67.9	49.2	0.3	-11.5	298.5	310.3	17.0	-17.8	-0.2	-0.6	88.4	6.4	6.2
	19940128	10.6	59.9	49.3	0.3	14.9	328.8	313.4	19.2	2.6	0.2	5.5	96.5	5.7	47.5
	20040203	11.8	117.1	105.4	0.4	-4.5	301.7	306.3	10.6	0.4	1.4	1.2	90.7	3.6	19.7
	Average	11.7	76.4	64.7	0.4	-0.1	311.3	311.4	17.1	-3.8	0.4	2.4	91.3	4.9	25.3
1032	19820219	20.5	74.2	53.7	0.3	-8.3	305.0	313.5	21.8	-19.6	0.3	1.4	80.1	4.4	14.7
	19850202	14.4	52.2	37.8	0.3	-9.1	305.3	314.7	8.1	-7.8	0.9	1.0	89.4	4.1	6.4
	19870223	20.7	73.9	53.2	0.3	-13.4	301.6	315.5	14.3	-2.5	0.9	2.5	74.2	5.2	20.0
	20021211	5.9	62.9	57.0	0.3	-13.9	287.9	302.1	31.3	-5.3	1.2	1.0	66.3	4.9	19.2
	20050221	24.3	88.2	63.9	0.4	-6.8	306.9	314.0	7.2	-1.9	0.5	1.6	87.1	3.3	23.3
	Average	17.2	70.3	53.1	0.3	-10.3	301.3	312.0	16.5	-7.4	0.8	1.5	79.4	4.4	16.7

Table 3.4. Results from a single factor ANOVA for net shortwave radiation (K_{net}), net longwave radiation (L_{net}), sensible (H), latent (LE), and ground (G) heat fluxes during ROS events.

		SS	df	MS	F	Sig.
K_{net}	Between groups	85.6	3	28.5	0.41	0.749
	Within groups	905.3	13	69.6		
	Total	991	16			
L_{net}	Between groups	830.4	3	276.8	1.15	0.366
	Within groups	3131.9	13	240.9		
	Total	3962.4	16			
H	Between groups	115.3	3	38.4	0.411	0.748
	Within groups	1216.5	13	93.6		
	Total	1331.7	16			
LE	Between groups	199.3	3	66.42	1.76	0.203
	Within groups	489.6	13	37.7		
	Total	688.9	16			
G	Between groups	0.686	3	0.229	0.693	0.572
	Within groups	4.286	13	0.33		
	Total	4.97	16			

Table 3.5. Average daily flux components (W m^{-2}) and albedo as well as modeled temperature (T, °C), relative humidity (RH, %) and wind speed (WS, m s^{-1}) for the common synoptic types associated with each event after all precipitation is removed from the model run as well as an average for each synoptic type.

	Date	K_{net}	K_d	K_u	a	L_{net}	L_d	L_u	H	LE	G	T	RH	WS	NET
Type 1004	19860218	13.1	137.3	124.2	0.4	-1.7	313.7	315.5	6.2	0.2	1.2	2.9	95.0	3.8	18.9
	20030222	13.6	141.6	128.1	0.5	-3.0	312.4	315.5	5.3	0.2	0.8	2.5	92.6	3.7	16.8
	20031214	6.8	72.8	66.1	0.3	-6.0	303.0	309.1	23.6	0.3	0.4	1.4	69.4	5.2	25.0
	20091226	7.9	80.2	72.3	0.3	21.0	337.2	315.5	16.4	1.2	1.2	7.5	96.5	6.4	47.6
	AVG	10.3	108.0	97.6	0.4	2.6	316.6	313.9	12.8	0.5	0.9	3.6	88.4	4.8	27.1
Type 1011	19880118	8.6	94.3	85.8	0.4	0.1	314.0	313.9	7.5	0.1	1.5	3.2	87.8	2.9	17.8
	19900108	8.3	85.4	77.1	0.4	-9.7	302.1	312.1	2.1	-0.9	0.6	0.6	88.9	2.5	0.4
	19960119	9.0	94.7	85.7	0.4	49.0	366.1	315.5	30.0	3.7	1.0	13.2	92.7	8.8	92.8
	20000219	13.3	136.9	123.7	0.5	-5.3	309.6	315.0	3.7	0.1	0.4	1.6	97.5	3.5	12.2
	AVG	9.8	102.8	93.1	0.4	8.5	322.9	314.1	10.8	0.8	0.9	4.7	91.7	4.4	30.8
Type 1031	19820203	10.7	113.6	103.0	0.4	0.7	316.1	315.3	21.8	-0.2	0.6	3.4	89.6	4.1	33.6
	19830207	11.6	118.9	107.2	0.4	-11.4	298.5	310.2	17.5	-17.0	0.0	-0.6	88.4	6.4	0.7
	19940128	10.1	105.0	94.9	0.4	15.4	329.2	313.2	22.0	4.1	0.7	5.6	96.2	5.7	52.2
	20040203	11.9	118.5	106.6	0.4	-4.5	301.7	306.3	10.6	0.4	1.4	1.2	90.7	3.6	19.8
	AVG	11.1	114.0	102.9	0.4	0.1	311.4	311.3	18.0	-3.2	0.7	2.4	91.2	4.9	26.6
Type 1032	19820219	13.5	138.6	125.1	0.4	-8.1	305.0	313.3	22.2	-18.5	0.4	1.4	80.1	4.4	9.5
	19850202	10.4	112.4	102.0	0.4	-9.3	305.3	314.9	7.1	-8.5	1.0	1.0	89.4	4.1	0.7
	19870223	18.9	163.0	144.1	0.4	-13.5	301.6	315.5	14.0	-2.6	0.9	2.5	74.2	5.2	17.8
	20021211	7.8	82.7	74.9	0.3	-13.8	287.9	302.0	32.0	-5.0	1.2	1.0	66.3	4.9	22.3
	20050221	13.5	140.8	127.4	0.5	-5.9	306.9	313.0	7.0	-1.3	0.8	1.6	87.1	3.3	14.1
	AVG	12.8	127.5	114.7	0.4	-10.1	301.3	311.7	16.5	-7.2	0.9	1.5	79.4	4.4	12.9

Table 3.6. Results from a paired sample for means t-Test for daily ground heat flux for Weak Carolinas Low (α=0.05).

	1004r	*1004x*
Mean	0.293	0.898
Variance	0.279	0.139
Observations	4	4
Pearson Correlation	0.931	
Hypothesized Mean Difference	0	
df	3	
t Stat	-5.33	
P(T<=t) one-tail	0.0064	
t Critical one-tail	2.35	
P(T<=t) two-tail	0.0128	
t Critical two-tail	3.18	

Table 3.7. Results from a paired sample for means t-Test for daily ground heat flux for Great Lakes Low (α=0.05).

	1031r	*1031x*
Mean	0.389	0.675
Variance	0.518	0.350
Observations	4	4
Pearson Correlation	0.959	
Hypothesized Mean Difference	0	
df	3	
t Stat	-2.53	
P(T<=t) one-tail	0.043	
t Critical one-tail	2.35	
P(T<=t) two-tail	0.086	
t Critical two-tail	3.18	

Table 3.8. Results from a paired sample for means t-Test for daily net shortwave radiation for the Mid-Atlantic Coastal Low (α=0.05).

	1032r	*1032x*
Mean	17.2	12.8
Variance	52.2	17.5
Observations	5	5
Pearson Correlation	0.763	
Hypothesized Mean Difference	0	
df	4	
t Stat	2.00	
P(T<=t) one-tail	0.058	
t Critical one-tail	2.13	
P(T<=t) two-tail	0.115	
t Critical two-tail	2.78	

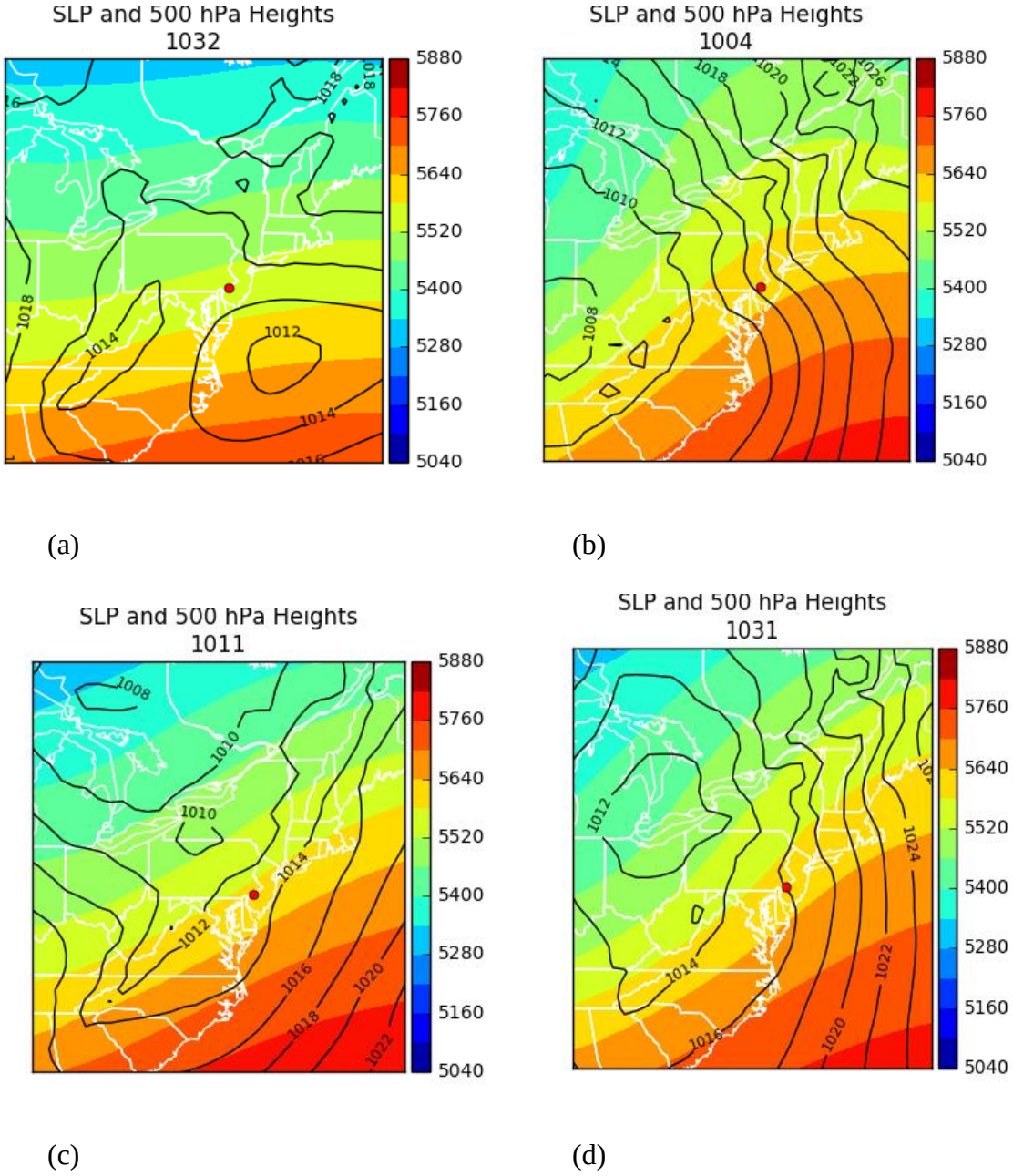

Figure 3.1. Composites of mean sea level pressure in hPa (black contours) and 500 hPa heights (filled contours) for a 00z to 00z period on ROS days for (a) the Mid-Atlantic Coastal Low (1032), (b) the Weak Carolinas Low (1004), (c) the New England Low (1011), and (d) the Great Lakes Low (1031). The red point indicates the location of KPHL.

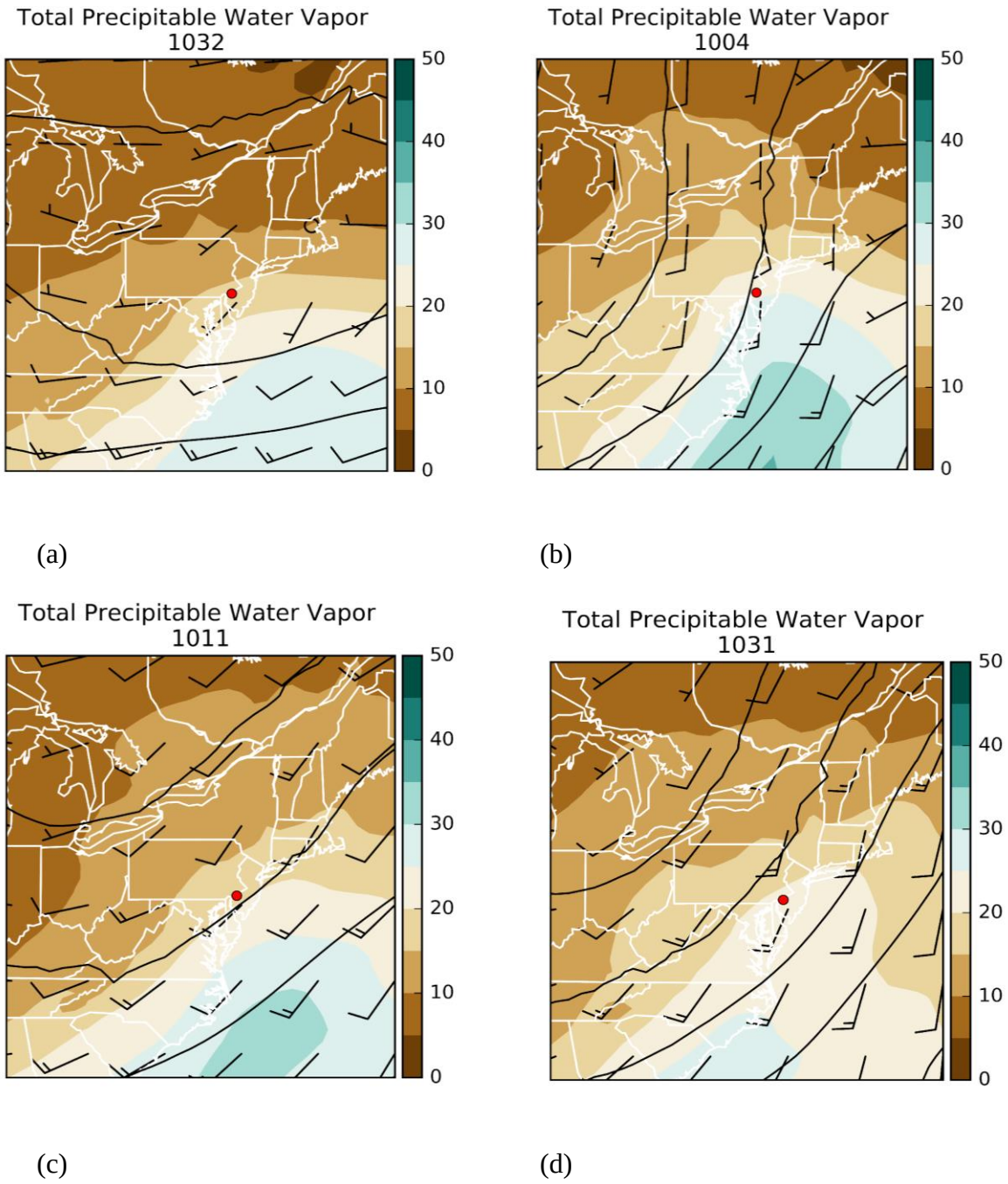

Figure 3.2. Composites of precipitable water vapor in mm (filled contours) and 850 hPa heights (black contours) and 850 hPa wind speed in m s^{-1} for the 00z to 00z period on ROS days for (a) the Mid-Atlantic Coastal Low (1032), (b) the Weak Carolinas Low (1004), (c) the New England Low (1011), and (d) the Great Lakes Low (1031). The red point indicates the location of KPHL.

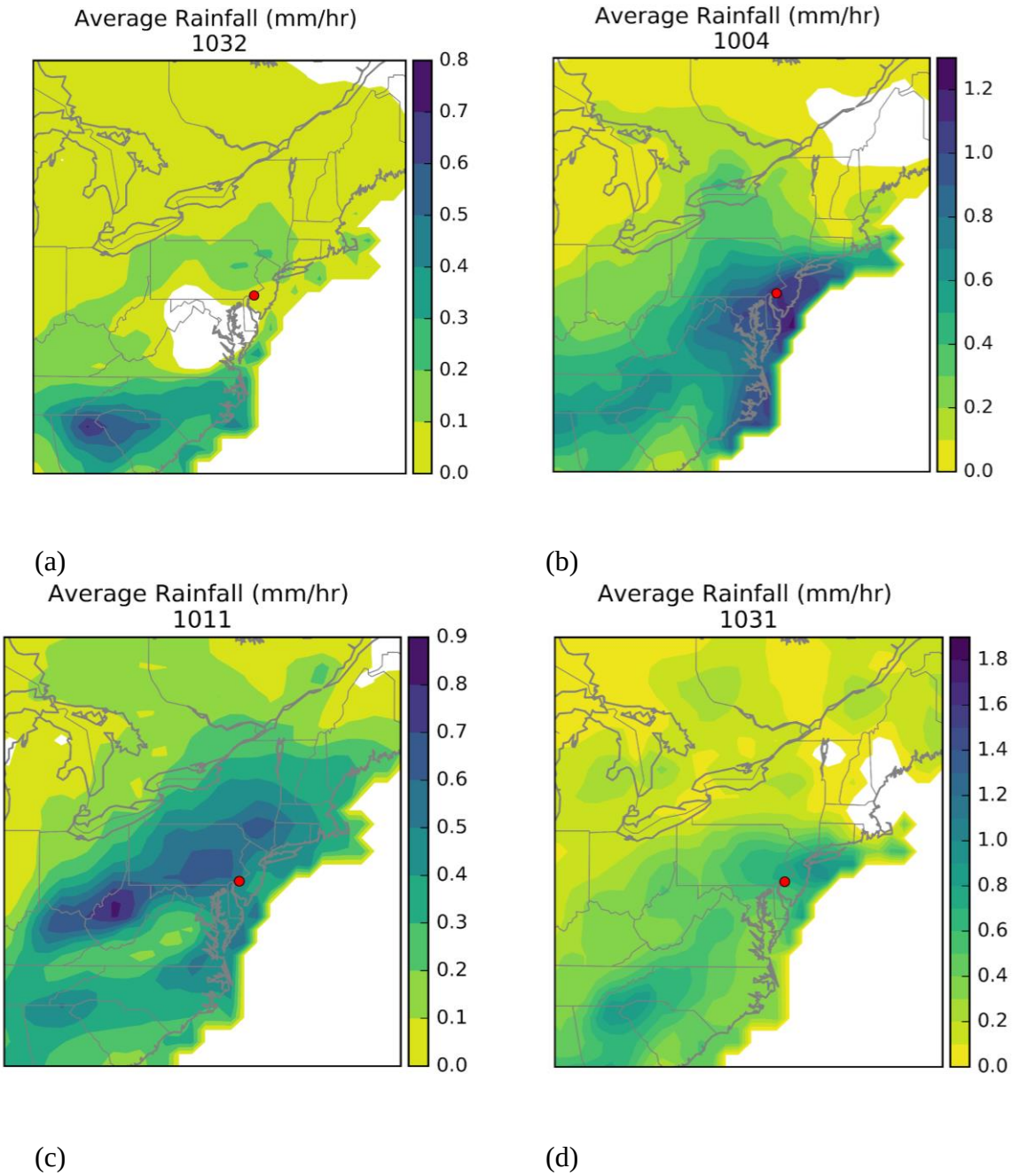

Figure 3.3. Average rainfall rates (mm hr^{-1}) for each synoptic type. Rainfall rates are estimated from MERRA-2 total precipitation land product minus total snowfall land product for (a) the Mid-Atlantic Coastal Low (1032), (b) the Weak Carolinas Low (1004), (c) the New England Low (1011), and (d) the Great Lakes Low (1031). The red point indicates the location of KPHL.

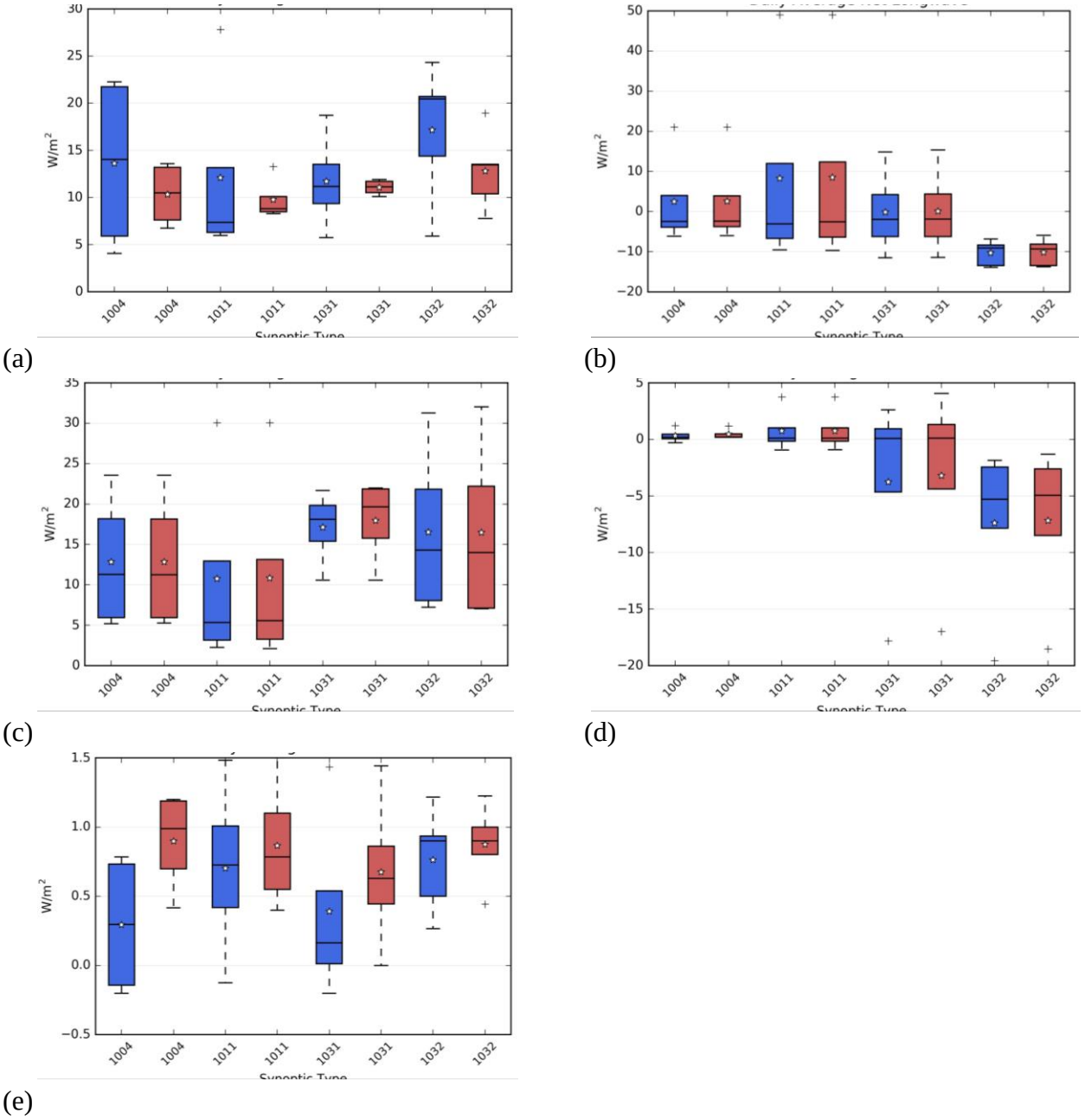

Figure 3.4. Average daily flux components for modeled rain (blue) and no-precipitation (red) events for the daily average (a) net shortwave radiative flux, (b) net longwave radiative flux, (c) sensible heat flux, (d) latent heat flux, and (e) ground heat flux (W m^{-2}). Positive flux values indicate energy flux directed toward the snowpack (e.g., heat added); negative values indicate energy directed away from the snowpack (e.g., heat lost). White star indicates the mean flux for each synoptic type.

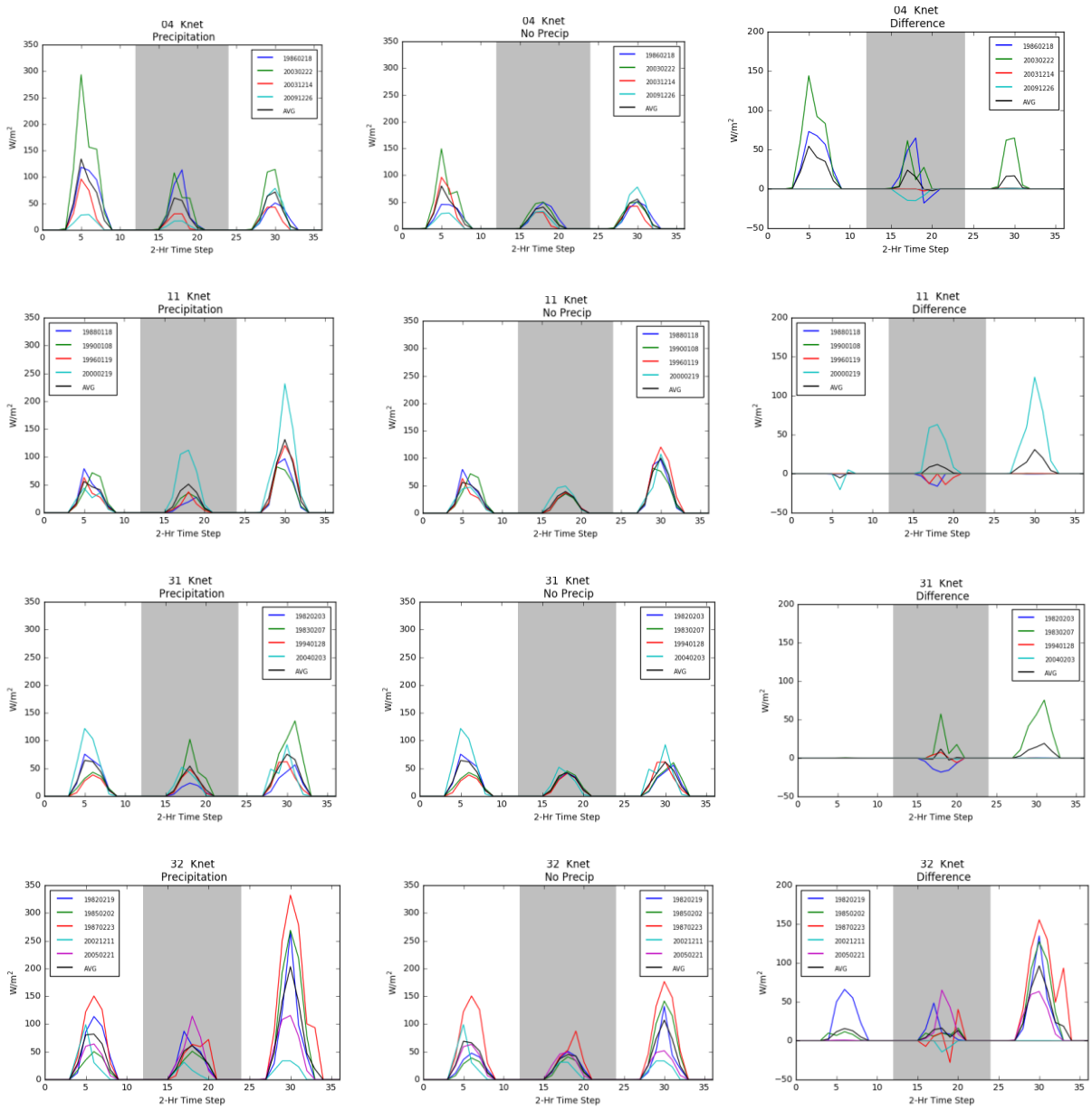

Figure 3.5. Time series of 2-hour SNTHERM output for net shortwave radiation (W m^{-2}) for each ROS event (left column), the no-precipitation scenario (center column), and the difference between the two scenarios, calculated as R – NP (right column); rows are broken up by synoptic type with Weak Carolinas Low (1004; top), New England Low (1011; second from top), Great Lakes Low (1031; second from bottom), and Mid-Atlantic Coastal Low (1032; bottom).

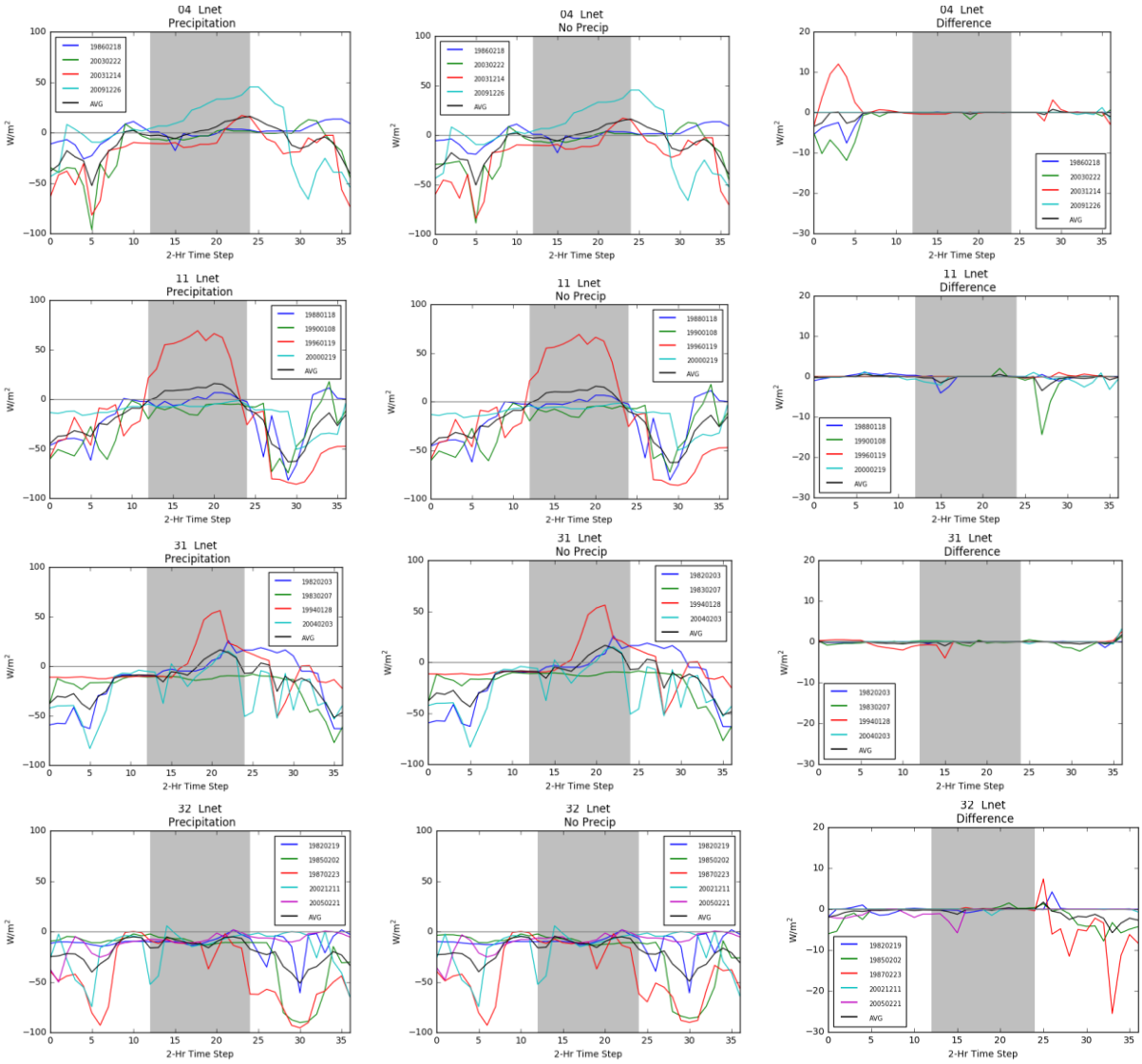

Figure 3.6. Time series of 2-hour SNTHERM output for net longwave radiation (W m^{-2}) for each ROS event (left column), the no-precipitation scenario (center column), and the difference between the two scenarios, calculated as R – NP (right column); rows are broken up by synoptic type with Weak Carolinas Low (1004; top), New England Low (1011; second from top), Great Lakes Low (1031; second from bottom), and Mid-Atlantic Coastal Low (1032; bottom).

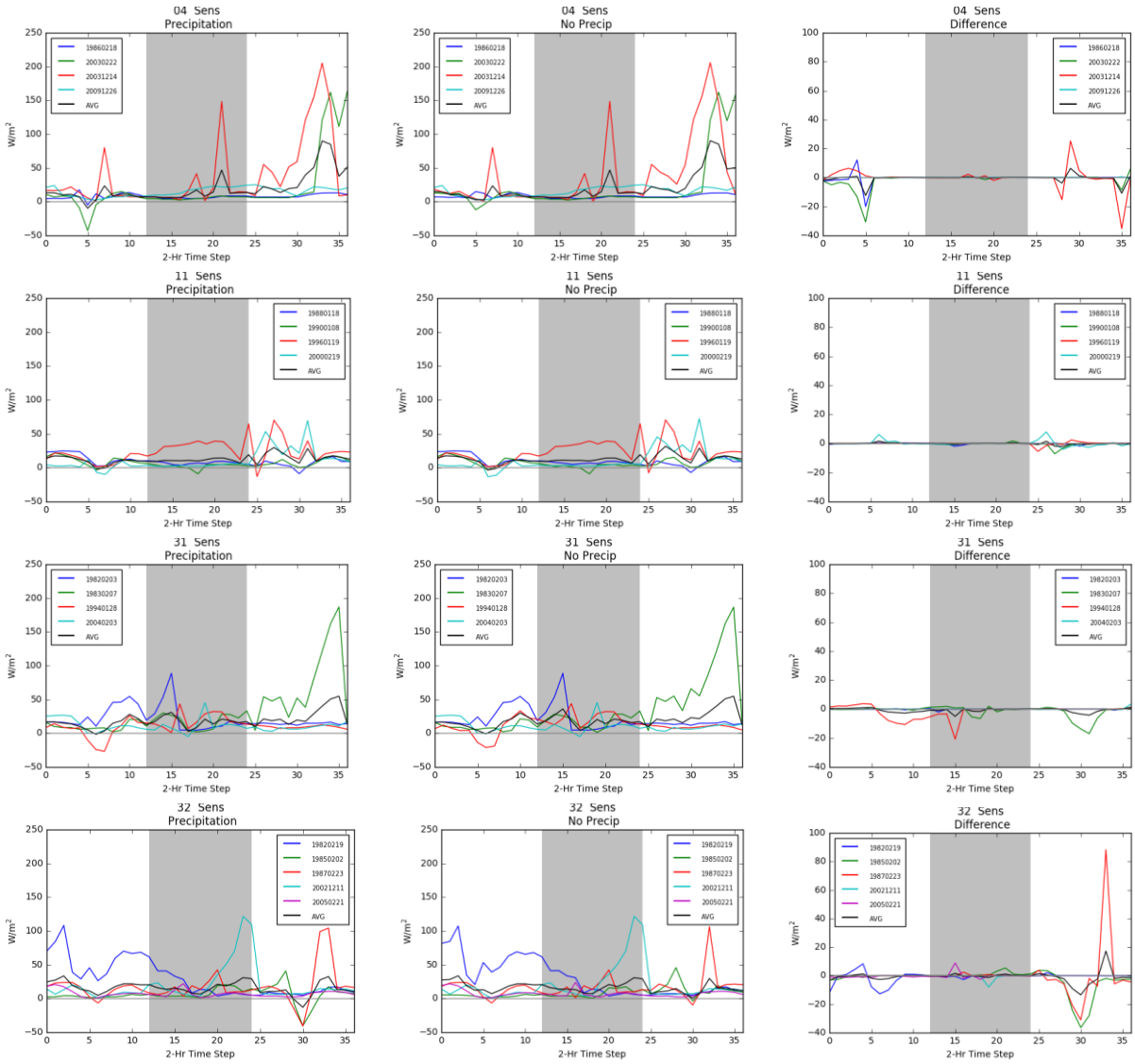

Figure 3.7. Time series of 2-hour SNTHERM output for sensible heat flux (W m^{-2}) for each ROS event (left column), the no-precipitation scenario (center column), and the difference between the two scenarios, calculated as R – NP (right column); rows are broken up by synoptic type with Weak Carolinas Low (1004; top), New England Low (1011; second from top), Great Lakes Low (1031; second from bottom), and Mid-Atlantic Coastal Low (1032; bottom).

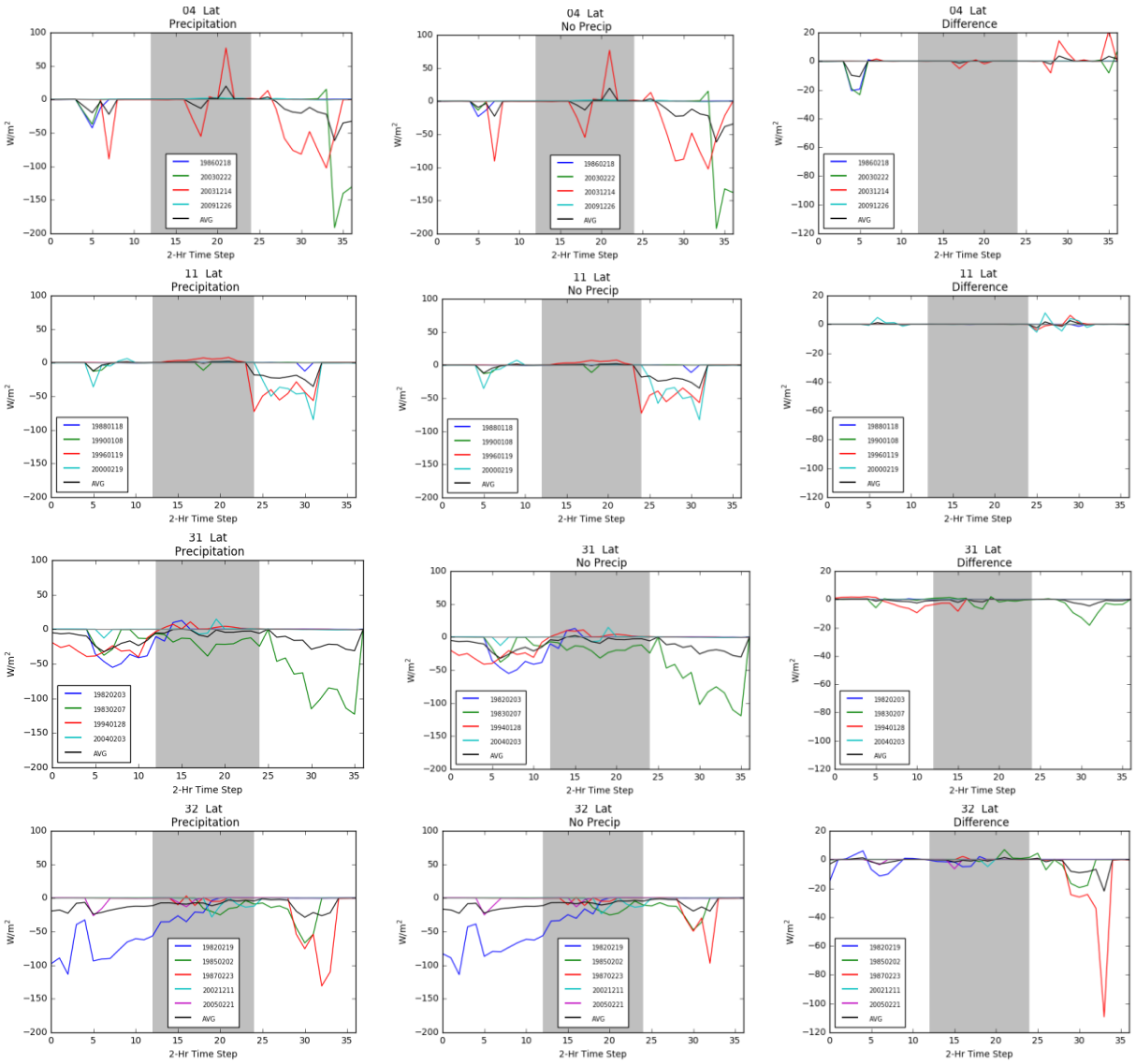

Figure 3.8. Time series of 2-hour SNTHERM output for latent heat flux (W m^{-2}) for each ROS event (left column), the no-precipitation scenario (center column), and the difference between the two scenarios, calculated as R – NP (right column); rows are broken up by synoptic type with Weak Carolinas Low (1004; top), New England Low (1011; second from top), Great Lakes Low (1031; second from bottom), and Mid-Atlantic Coastal Low (1032; bottom).

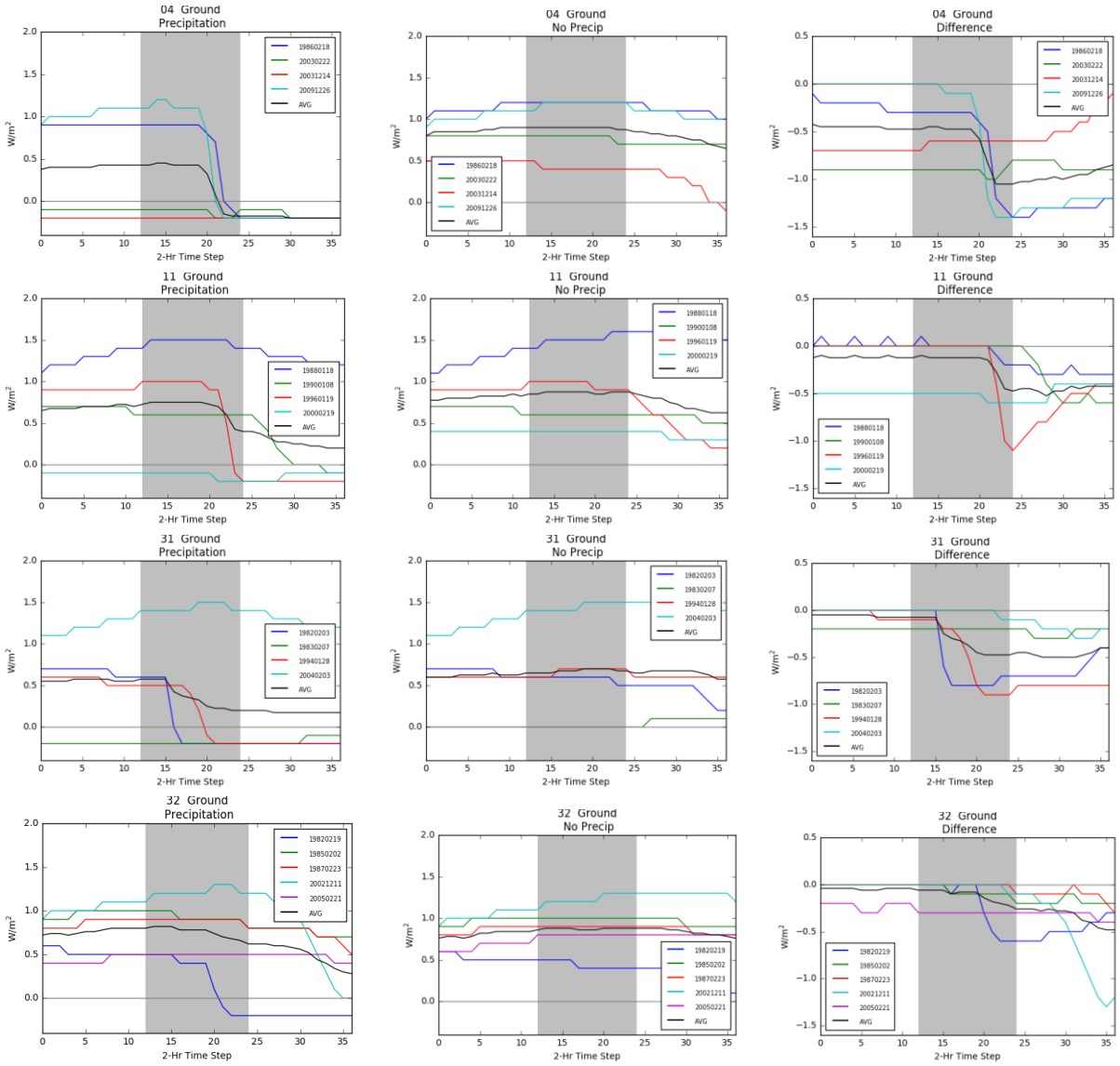

Figure 3.9. Time series of 2-hour SNTHERM output for ground heat flux (W m^{-2}) for each ROS event (left column), the no-precipitation scenario (middle column), and the difference between the two scenarios, calculated as R – NP (right column); rows are broken up by synoptic type with Weak Carolinas Low (1004; top), New England Low (1011; second from top), Great Lakes Low (1031; second from bottom), and Mid-Atlantic Coastal Low (1032; bottom).

CHAPTER 4

CONCLUSION

This thesis addresses rain-on-snow (ROS) in the eastern United States, with focus on the mid-Atlantic region. In particular, differences in spatial and temporal characteristics in a ROS climatology as a function of event selection are examined. Furthermore, differences in the surface energy budget (SEB) during ROS are discussed, with primary focus on changes in the SEB resulting from the presence of rain.

When identifying ROS events during 1960–2009, the use of four different selection criteria (i.e., "definitions") showed a large change in the total number of events for a location (by season), as well as number events occurring per year. Geographic areas in which more events were present was generally similar across definitions; however, localized maxima tended to remain in higher latitude and/or higher elevations for a more generic definition as well as for the definition focusing primarily on snow depth loss. For definitions including higher rainfall amounts, more events were recorded along the U.S. east coast. ROS events defined by more strict criteria regarding rainfall and loss of snow depth were also more common in Maine. More events occurred during the spring, although localized maxima tend to vary depending on season.

A selection of three locations (i.e., Philadelphia, PA; Buffalo, NY; and Flint, MI) to assess temporal trends in ROS throughout the mid-Atlantic show that Buffalo experienced ROS events most frequently, regardless of how the events are identified; Flint experienced the second-most the most inclusive ROS criteria, but the fewest events using the three other definitions assessed. Of the three cities examined in detail, Philadelphia had the fewest number of ROS

events with the most inclusive definition, but had the highest percentage (~12.5%) of the events with greater rainfall and a larger magnitude of snow depth loss compared to Buffalo and Flint (each with 5–6% of the total events categorized as D4). This finding suggests that ROS events in near-coastal locations may be influenced by storms conducive to more temperature and/or moisture advection, as the warmer ocean may be providing these sources to the region.

Additionally, when considering the number of events per year, there was an apparent decrease in the number of ROS events for both Buffalo and Flint, likely due to the decreasing seasonal snowpack. No trend was apparent for Philadelphia.

Given the higher frequency of more impactful ROS events in Philadelphia as well as its close proximity to the coastline, ROS events meeting the >1 cm rainfall criteria between 1980–2009 are further analyzed in terms of their energy budget and synoptic-scale atmospheric circulation. Using the Temporal Synoptic Index (TSI), synoptic-scale circulation patterns matching those of an approaching surface cyclone were commonly associated with ROS. In particular, while more ROS events were common with a colder, drier air mass, a higher percentage of days where a warmer and more moist air mass was present resulted in ROS in Philadelphia, synoptic-scale composites using MERRA-2 reanalysis data show the placement of this cyclone was conducive to larger amounts of warm air and moisture advection.

Station data from Philadelphia were used to drive SNTHERM in order to derive the SEB during these ROS events. While no significant model-derived SEB variations attributed to synoptic types were present, variations within each synoptic type suggest other influences (e.g., snowpack characteristics) which may need to be considered. Moreover, as each common synoptic type consisted of 4-5 events, more events should be analyzed in future work.

From a sensitivity analysis, SNTHERM simulations without any precipitation compared to the ROS scenarios showed the influence of rain typically played a role in influencing parts of the SEB. Rain acted to change the albedo of the surface of the snowpack, which influenced net shortwave radiation to an extent; however, atmospheric circulation patterns frequently associated with stronger warm air and moisture advection showed the presence of rain could significantly change the ground heat flux during ROS. As rain percolates through the snowpack, some of it refreezes, releasing heat and aiding in ripening the snowpack. As the ground is frozen, the temperature gradient between the warmer snowpack and the colder ground weakens the heat flux from the ground. Moreover, ROS events associated with the cooler, drier synoptic type showed rainfall changing the surface albedo of the snowpack, which influenced net shortwave radiation.

The results provide a first attempt at quantified the SEB during ROS events as a function of synoptic type in the eastern US. From these results, future ROS events should first consider how events will be selected and whether this selection criteria is appropriate for regional-scale studies on ROS, given the inter-regional scale of spatial and temporal variability of these events. Moreover, it has been shown that the degree of moisture transport into the mid-Atlantic region tends to play a role during ROS. This should motivate future work into establishing relationships between significant ROS events and magnitude of moisture transport, particularly in this region as an apparent absence of this type of work is missing in the literature.

REFERENCES

Anderson, E., and L. Larson, 1996: The role of snowmelt in the January 1996 floods in the northeastern United States. *Proc. 53d Eastern Snow Conference, Eastern Snow Conference*, Williamsburg, VA, 141–149.

Ashley, S. T. and W. S. Ashley, 2008: The storm morphology of deadly flooding events in the United States. *Int. J. Climatol*., **28**, 493–503, doi:10.1002/joc.1554.

Cohen, J., H. Ye, and J. Jones, 2015: Trends and variability in rain-on-snow events, *Geophys. Res. Lett.,* **42**, 7115–7122, doi:10.1002/2015GL065320.

Collins, M. J., J. P. Kirk, J. Pettit, A. T. DeGaetano, M. S. McCown, T. C. Peterson, T. N. Means, and X. Zhang, 2014: Annual floods in New England (USA) and Atlantic Canada: synoptic climatology and generating mechanisms, *Phys. Geogr.*, **35**, 195-219.

Dyer, J. L., and T. L. Mote, 2006: Spatial variability and trends in observed snow depth over North America. *Geophys. Res. Lett*., **33**, L16503, doi:10.1029/2006GL027258.

Freudiger, D., I. Kohn, K. Stahl, and M. Weiler, 2014: Large-scale analysis of changing frequencies of rain-on-snow events with flood-generation potential, *Hydrol. Earth Syst. Sci.,* **18**, 2695-2709.

Garvelmann, J., S. Pohl, and M. Weiler, 2014: Variability of observed energy fluxes during rain-on-snow and clear sky snowmelt in a midlatitude mountain environment, *J. of Hydrometeor.,* **15**, 1220-1237.

Gelaro, R., W. McCarty, M. J. Suárez, R. Todling, A. Molod, L. Takacs, et al., 2017: The modern-era retrospective analysis for research and applications, version 2 (MERRA-2). *J. of Clim.*, **30**, 5419-5454.

Graybeal, D. Y., and D. J. Leathers, 2006: Snowmelt-related flood risk in Appalachia: first estimates from a historical snow climatology, *J. of Appl. Meteor. Climatol.,* **45**, 178-193.

Grundstein, A. J., and D. J. Leathers, 1999: A spatial analysis of snow-surface energy exchanges over the northern Great Plains of the United States in relation to synoptic scale forcing mechanisms, *Int. J. Climatol.,* **19**, 489-511.

Grundstein, A., T. Mote, and D. Leathers, 2002: A hybrid climatology of snow water equivalent over the northern Great Plains of the United States, *Polar Geogr.*, **26**, 187-209.

Guan, B., D. E. Waliser, F. M. Ralph, E. J. Fetzer, and P. J. Neiman, 2016: Hydrometeorological Characteristics of Rain-on-Snow Events Associated with Atmospheric Rivers, *Geophys. Res. Lett.,* **43**, 2964-2973.

Jennings, K. and J. A. Jones, 2015: Precipitation-snowmelt timing and snowmelt augmentation of large peak flow events, western Cascades, Oregon, *Water Resour. Res.*, **51**, 7649-7661.

Jeong, D. I., and L. Sushama, 2017: Rain-on-snow events over North America based on two Canadian regional climate models, *Clim. Dyn.*, 1-14.

Jordan, R., 1991: A one-dimensional temperature model for a snow cover: Technical documentation for SNTHERM.89. Special Report 91-16, 49 pp. [Available from U.S. Army Corps of Engineers, Cold Regions Research and Engineering Laboratory, Hanover, NH 03755.].

Kalkstein, L. S., and P. Corrigan, 1986: A synoptic climatological approach for geographical analysis: assessment of sulfur dioxide concentrations, *Ann. Assoc. Am. Geogr.,* **76**, 381-395.

Kluver, D., T. Mote, D. Leathers, G. R. Henderson, W. Chan, and D. A. Robinson, 2016: Creation and validation of a comprehensive 1 by 1 daily gridded North American dataset for 1900–2009: snowfall, *J. Atmos. Oceanic Technol.*, **33**, 857-871.

Kroczynski, S., 2004: A comparison of two rain-on-snow events and the subsequent hydrologic responses in three small river basins in Central Pennsylvania, Eastern Region Technical Attachment, **4**, 1–21.

Leathers, D. J., D. Graybeal, T. Mote, A. Grundstein, and D. Robinson, 2004: The role of airmass types and surface energy fluxes in snow cover ablation in the central Appalachians, *J. of Appl. Meteor. Climatol.,* **43**, 1887-1899.

Leathers, D. J., D. R. Kluck, and S. Kroczynski, 1998: The severe flooding event of January 1996 across north-central Pennsylvania, *Bull. Am. Meteor. Soc.,* **79**, 785.

Marks, D., J. Kimball, D. Tingey, and T. Link, 1998: The sensitivity of snowmelt processes to climate conditions and forest cover during rain-on-snow: a case study of the 1996 Pacific Northwest flood, *Hydrol. Process*., **12**, 1569-1587.

McCabe, G. J., L. E. Hay, and M. P. Clark, 2007: Rain-on-Snow Events in the Western United States, *Bull. Amer. Meteor. Soc*., **88**, 319–328. doi: 10.1175/BAMS-88-3-319.

Mazurkiewicz, A. B., D. G. Callery, and J. J. McDonnell, 2008: Assessing the controls of the snow energy balance and water available for runoff in a rain-on-snow environment, *J. Hydrol.*, **354**, 1-14.

Pradhanang, S. M., A. Frei, M. Zion, E. M. Schneiderman, T. S. Steenhuis, and D. Pierson, 2013: Rain-on-snow runoff events in New York, *Hydrol. Process.*, **27**, 3035-3049.

Putkonen, J., T. C. Grenfell, K. Rennert, C. Bitz, P. Jacobson, and D. Russell, 2009: Rain on snow: little understood killer in the north, *Trans., Am. Geophys. Union*, **90**, 221-222.

Rössler, O., P. Froidevaux, U. Börst, R. Rickli, O. Martius, and R. Weingartner, 2014: Retrospective analysis of a non-forecasted rain-on-snow flood in the Alps–a matter of model limitations or unpredictable nature, *Hydrol. Earth Syst. Sci*, **18**, 2265-2285.

Surfleet, C. G., and D. Tullos, 2013: Variability in effect of climate change on rain-on-snow peak flow events in a temperate climate, *J. Hydrol.*, **479,** 24-34.

Suriano, Z. J., and D. J. Leathers, 2017: Spatiotemporal Variability of Great Lakes Basin Snow Cover Ablation Events, *Hydrol. Process.*, 1–9.

Suriano, Z. J., and D. J. Leathers, 2017: Synoptically classified lake-effect snowfall trends to the lee of Lakes Erie and Ontario, *Clim. Res.*, **74,** 1-13.

Suriano, Z.J. and D.J. Leathers, 2017: Synoptic climatology of lake-effect snowfall condition in the eastern Great Lakes region, *Int. J. Climatol.*, **37**, 4377-4389. doi: 10.1002/joc.5093.

Ye, H., D. Yang, and D. Robinson, 2008: Winter rain on snow and its association with air temperature in northern Eurasia, *Hydrol. Process.*, **22**, 2728-2736.